A STATISTICAL ANALYSIS OF EMISSION-LINE MEMBERS OF THE ORION POPULATION

Joe Lee Frank

THESIS

A STATISTICAL ANALYSIS OF EMISSION-LINE MEMBERS OF THE ORION POPULATION

by

Joe Lee Frank III

December 1975

Thesis Advisor: William B. Zeleny

Unclassified

SECURITY CLASSIFICATION OF THIS PAGE (When Date Entered)

REPORT DOCUMENTATION PAGE		READ INSTRUCTIONS BEFORE COMPLETING FORM
1. REPORT NUMBER	2. GOVT ACCESSION NO.	3. RECIPIENT'S CATALOG NUMBER
4. TITLE (and Subtitle) A Statistical Analysis of Emission-Line Membersof the Orion Population		5. TYPE OF REPORT & PERIOD COVERED Master's Thesis; December 1975 6. PERFORMING ORG. REPORT NUMBER
7. AUTHOR(s) Joe Lee Frank III		8. CONTRACT OR GRANT NUMBER(s)
9. PERFORMING ORGANIZATION NAME AND ADDRESS Naval Postgraduate School Monterey, California 93940		10. PROGRAM ELEMENT, PROJECT, TASK AREA & WORK UNIT NUMBERS
11. CONTROLLING OFFICE NAME AND ADDRESS Naval Postgraduate School Monterey, California 93940		12. REPORT DATE 13. NUMBER OF PAGES
14. MONITORING AGENCY NAME & ADDRESS(if different from Controlling Office) Naval Postgraduate School Monterey, California 93940		15. SECURITY CLASS. (of this report) Unclassified 15a. DECLASSIFICATION/DOWNGRADING SCHEDULE

16. DISTRIBUTION STATEMENT (of this Report)

Approved for public release; distribution unlimited.

17. DISTRIBUTION STATEMENT (of the abstract entered in Block 20, if different from Report)

18. SUPPLEMENTARY NOTES

19. KEY WORDS (Continue on reverse side if necessary and identify by block number)

T Tauri stars

Orion Population

Emission line stars

Pre-main sequence stellar evolution

20. ABSTRACT (Continue on reverse side if necessary and identify by block number)

A statistical analysis of the "Second Catalog of Emission-Line Stars of the Orion Population" was undertaken. After the reduction of the Catalog to numeric data, statistics and frequency distributions were systematically searched for any physically significant characteristics. Those two-way frequency distributions with possible physical significance were analyzed.

Distance moduli for 228 stars were tabulated. Hertzsprung-Russell diagrams were plotted. The T Tauri stars, so plotted,

DD FORM 1 JAN 73 1473 EDITION OF 1 NOV 68 IS OBSOLETE
S/N 0102-014-6601 |
(Page 1)

Unclassified

SECURITY CLASSIFICATION OF THIS PAGE (When Date Entered)

lic between the main sequence and giant branch. A lack of correlation between the large scale variability and any other set of observed characteristics was discovered. Present theories of stellar evolution do not explain this lack of correlation nor the cause of the variability. It is argued, that on the basis of current data, no conclusion can be reached as to whether T Tauri stars are on convective or radiative equilibrium tracks approaching the main sequence. A luminosity function for the Orion Population is presented and is found to be significantly different than the solar neighborhood luminosity function.

A Statistical Analysis of Emission-Line Members of the Orion Population

by

Joe Lee Frank III
Lieutenant, United States Navy
B.S., United States Naval Academy, 1968

Submitted in partial fulfillment of the
requirements for the degree of

MASTER OF SCIENCE IN PHYSICS

from the

NAVAL POSTGRADUATE SCHOOL

December 1975

ABSTRACT

A statistical analysis of the "Second Catalog of Emission-Line Stars of the Orion Population" was undertaken. After the reduction of the Catalog to numeric data, statistics and frequency distributions were systematically searched for any physically significant characteristics. Those two-way frequency distributions with possible physical significance were analyzed.

Distance moduli for 228 stars were tabulated. Hertzsprung-Russell diagrams were plotted. The T Tauri stars, so plotted, lie between the main sequence and giant branch. A lack of correlation between the large scale variability and any other set of observed characteristics was discovered. Present theories of stellar evolution do not explain this lack of correlation nor the cause of the variability. It is argued, that on the basis of current data, no conclusion can be reached as to whether T Tauri stars are on convective or radiative equilibrium tracks approaching the main sequence. A luminosity function for the Orion Population is presented and is found to be significantly different than the solar neighborhood luminosity function.

TABLE OF CONTENTS

LIST OF TABLES

LIST OF FIGURES

ACKNOWLEDGEMENT

My special thanks to Dr. William Bruce Weaver who, though not a member of the Naval Postgraduate School Faculty, provided the guidance and encouragement as my advisor to bring this research to a successful completion.

The Monterey Institute for Research in Astronomy (MIRA) made their library available to me; and the professional staff astronomers were helpful in answering my questions. As this research was the first interaction between the Naval Postgraduate School and MIRA, it is my hope that it will be the start of a long period of cooperation and mutual benefit.

Mr. Robert Batesole and Associate Professor Donald R. Barr of the Postgraduate School gave great assistance in some of the more difficult statistical analyses.

I. INTRODUCTION

The dynamics and evolution of stars in hydrostatic equilibrium fusion cores is well understood. There is relatively good agreement between theory and observations on stellar age, composition, luminosity and effective temperature, and stability of these objects. Many observations support these theories that predict: shorter lifetimes for more massive stars; evolution of giant and supergiant stars; production of planetary nebulae, novae, and super novae; and collapse to white dwarfs and neutron stars. It is possible that even the final stage of stellar evolution (for some stars), the black hole, has been indirectly observed.

No such set of matching observations and theories exist for newly formed stars. Several theories have been suggested which predict the details of collapse for dense clouds of interstellar gas and dust, under highly idealized conditions. But observational support for many of the gross physical details of these schemes has not been found. One prediction of the theories of early stellar evolution is the appearance of luminous young stars. The stars at the time of the appearance are predicted to have luminosities greater than main sequence stars of the same effective temperature. If stars, whose pre-main sequence nature can be determined are studied, then their observed properties can be used to distinguish between, or even challenge the basic features of existing

theories of early stellar evolution. The T Tauri stars seem to be such a group, by reason of their Hertzsprung-Russell diagram position, spectral peculiarities, and other unusual properties.

The first recognition of the homogeneous group of irregular variable (in apparent magnitude) stars was made by Joy [1945]. Eleven stars were included in that group, including the prototype star T Tauri, for which the group is named. Although no two of the T Tauri stars are exactly alike, Joy noted four characteristics that distinguish T Tauri variables from the multitude of other variable stars. These are: "(1) rapid irregular light-variations of about three magnitudes; (2) spectral type F5-G5, with emission lines resembling those of the solar chromosphere, particularly in the great strength of H and K of calcium; (3) low luminosity; (4) association with dark or bright nebulosity." In intervening years, these stars have come to be accepted as pre-main sequence objects.

Objective prism surveys since then have increased the number of known T Tauri stars to more than three hundred, including many stars which because of their association with nebulosity, emission-line spectra, and irregular light variations are T Tauri-like even though they are not strictly T Tauri stars by Joy's criteria. Herbig [1962] suggested that this overall set of emission and irregular variable stars be referred to as the "Orion Population." By 1972, Herbig and Rao [1972] were able to catalog 323 stars in the

"Orion Population," most of which are T Tauri stars. Although the information is incomplete for some stars, the Catalog, as the Herbig-Rao, 1972, paper will hereafter be called, includes data for the categories listed in Table I. Concurrently in the table, the Fortran variable name assigned to the particular characteristic is listed. These Fortran names are sometimes used in later discussions of the Catalog data. The program undertaken was to calculate the distributions and relationships among the categories in the Catalog.

II. BACKGROUND OF THE T TAURI PHENOMENA

A deeper discussion of the properties of member stars of the Orion Population and how these properties complement current understanding of pre-main sequence stellar evolution will be helpful in analyzing the Catalog data and uncovering important statistical relationships. The observed properties of Orion Population stars are limited to the spectra, photometry, light curves, positions and motions. Far too few are known members of binary systems to make the special techniques of binary studies especially useful in the analysis of the Catalog objects. With the spectra and photometry it is, however, possible in some cases to infer the mass, luminosity, composition, dynamics and age of the Orion Population objects.

A. OBSERVED PROPERTIES OF T TAURI AND T TAURI-LIKE STARS

It is currently believed that all stars evolve through a T Tauri-like stage. Computations of stellar models show that massive objects evolve more quickly than less massive ones; for example, a star of one solar mass will take about ten times as long to evolve to the main sequence as a star of five solar masses. The main sequence is a locus of points on a Hertzsprung-Russell diagram; the points' positions being defined by the luminosities and effective surface temperatures of stars which have evolved to equilibrium burning of hydrogen in the stellar core. Assuming that the ratios of

the numbers of stars of different masses, formed in our region of the galaxy, remains essentially constant with respect to time; then the number of low mass pre-main sequence (PMS) stars which can be observed is far more numerous than the number of larger mass objects, since the massive objects spend far less time in the PMS stage. Consequently, the largest group of stars in the Catalog are certain T Tauri stars (39.3%) or presumed so (9.9%). The other categories with hot members of spectral classes B and A, late-type low luminosity members and peculiar stars make up only 16% of the Catalog. About 35% of the Catalog stars are not currently classed at all but share some characteristics. A thorough discussion of the T Tauri stars follows, while the others are very similar and a brief discussion will suffice.

1. Observed Properties

In the following paragraphs the observed properties of T Tauri stars are discussed.

a. The Spectra

Much more is now known about T Tauri spectra than was reported in the initial establishment of the class of T Tauri stars [Joy, 1945]. The nature of the star's spectrum is singly the most important characteristic for inclusion as a T Tauri star. All the other characteristics are secondary, although necessary. A thorough discussion and delineation of T Tauri criteria is contained in a review article by Herbig [1962]. The following characteristics are observed in the spectrum:

(1) Emission Lines. Numerous emission lines are visible. These include hydrogen's (HI) Balmer lines, the H and K lines of once ionized calcium (Ca II), and in varying degrees lines of iron (Fe I, Fe II), titanium (Ti II) and forbidden lines of oxygen ([OI]) and sulphur ([S II]). Only in late T Tauri stars, may the helium (He I) be prominent. The hydrogen and calcium lines are the strongest in intensity, followed by the iron (Fe II) and titanium (Ti II) lines.[1]

(2) Underlying Spectrum. The emission lines of the previous paragraph are superimposed on either a continuous emission spectrum or in some cases a nearly normal photospheric absorption spectrum whose type ranges from F to M. The absorption lines may be considerably broadened. In those stars with an absorption spectrum, there is often a line of lithium (Li I 6707) which might legitimately be included as a criteria [Kuhi, 1966]. In general, the transition from an absorption spectrum to continuous emission masking absorption is most striking in the stars with strong emission lines. When definite lines appear, it is often possible to measure doppler shifts separate from those caused by the overall radial motion of the star. This overall radial motion must be inferred from the radial motion of associated stars in the same cluster.

---

[1]The Roman Numeral I indicates the neutral atom, II indicates the first ion, etc.; and the square brackets [ ] indicate forbidden transitions.

(3) P Cygni Profiles. Nearly all the T Tauri stars in which the absorption lines are visible have the lines arranged so that there is an obvious profile like that of P Cygni. This arrangement consists of an emission line symmetric in intensity about the central frequency with an absorption line bounding the emission just to the higher frequency (blue) side [Ambartsumyan, 1958]. The exceptions show an inverse P Cygni profile, that is, the absorption is to the lower frequency (red) side of the emission line [Walker, 1972]. These P Cygni features appear at the Balmer lines and the H and K Ca II lines.

(4) Ultraviolet Excess. There may be an ultraviolet (UV) excess and sometimes a "blue continuum" which has been interpreted as Balmer continuum radiation [Strom, Strom, and Grasdalen, 1975]. This causes masking, as mentioned previously, or as it is more commonly called, "veiling." It may be characterized by a steep rise in the spectral energy distribution shortward of about 4200 Å.

b. Polarization

Variable optical polarization as high as 12% has been observed. It is possibly caused by electron or dust scattering [Strom, Strom, and Grasdalen, 1975].

c. Infrared (IR) Excesses

Unusually intense IR radiation in the 1-3μ region was first noted by Mendoza [1966, 1968]. This IR emission is clearly greater than that which was expected from fitting a black body energy distribution to the intensities at visual wavelengths [Rydgren, Strom, and Strom, 1975].

d. Irregular Variability

Irregular variability in brightness was one of Joy's original criteria. Continuing analysis in the past thirty years has failed to uncover any underlying periodicity, except for a very few stars in which the time of independent characteristic cycles might have been found. The range of variability extends from differences of 0.2 magnitudes to 5.8 magnitudes. The mean and median range is about two magnitudes. The periods range from several days to several hundred days and more. There is variability in the infrared also [Mendoza, 1968], but which does not necessarily follow the changes in the visual wavelengths [Cohen, 1973a].

e. Association with Nebulosity

All of the stars appear close to nebulosity. Of the T Tauri stars, 13.8% illuminate or excite bright nebulosity. Herbig [1962] has shown that it is very unlikely that these stars are just ones which have been trapped by the nebulous clouds. The nebulosity tends to be heavy and total obscuration of other Orion Population objects is likely [Strom, Strom, and Grasdalen, 1975]. With IR surveys and searches, many more IR sources and likely T Tauri stars are being found. It must be noted that not all areas of great nebulosity have associated T Tauri stars.

f. O and B Associations

T Tauri stars do appear with some regularity in concentrations with O and B stars. The Orion Nebula is the most notable example. Because of their short lifetimes

the O and B stars must be young, and the observation that the T Tauri stars appear regularly close by is an important one. It must be pointed out, however, that not all groups of O and B stars have the associated T Tauri stars, the Pleiades being the most notable example. These points are discussed more fully by Kuhi [1966].

g. Non-T Tauri Stars in the Orion Population

The few stars which cannot be classified as T Tauri stars usually differ in their hot or peculiar spectra. But they usually share the emission characteristics, irregular variability, P Cygni profiles and IR excesses of the T Tauri stars. The hot members of the Orion Population and other non-T Tauri PMS objects are discussed by Strom, Strom, and Grasdalen [1975].

B. INFERRED PROPERTIES

In addition to its importance as a classification criterion, the spectrum of a T Tauri star yields the greatest information about those properties which are not directly observable, but which must be inferred or calculated from the observational evidence. This paper cannot deal in depth with the calculation or even estimation of all the characteristics and dynamics of a T Tauri star. Only the currently held conclusions will be given.

When a photospheric absorption spectrum can be resolved or when an intrinsic color can be obtained, the surface temperature may be defined to about two significant figures. If the distance to the star is known and an appropriate

correction for interstellar (and circumstellar) absorption can be applied, then an absolute magnitude and luminosity can be calculated from the apparent magnitude. There is a relationship between mass and luminosity, since the mass and composition uniquely determine all the physical characteristics of a star. But T Tauri stars may not be static, equilibrium objects. For those few stars for which physical characteristics can be estimated, the luminosity is greater than what is expected for a main sequence star. One might well conclude that the radius is greater than a main sequence object of equivalent mass.

These relationships discussed above can be described by a two-dimensional plot called the Hertzsprung-Russell (H-R) diagram. The abscissa of such a plot is appropriate units of either spectral class, color or temperature; the ordinate is absolute magnitude or luminosity. Radius might be added as a third non-orthogonal coordinate. Historical paths of stars of a particular mass can be plotted on the H-R diagram. Age then is a parameter. In addition, particular studies of binary systems may yield and/or confirm information about masses and radii. Also, there are indirect ways to calculate mass from estimates of surface gravity when good spectra are available.

Good spectra of T Tauri stars are exceedingly difficult to obtain as the objects are dim and the spectra are confused and often masked. So, with this brief background, the current beliefs concerning the T Tauri properties follow.

1. Physical Characteristics

The range of spectral classes has been discussed. Consequently, the range of temperatures for T Tauri stars follows directly, from about 6600°K to 2800°K [Allen, 1973]. These are effective black body temperatures. The intrinsic color $(B - V)_o$ likewise ranges from 0.4 to 1.6 magnitudes.

The radii are not at all well determined, but average in the neighborhood of several solar radii or greater.

The mass of the T Tauri stars probably range from 0.2 to 3 solar masses, but there is occasional excellent evidence for larger mass T Tauri stars [Strom, Strom, and Grasdalen, 1975]. There are certainly stars of clearly greater mass which exhibit T Tauri-like emission and variability.

The question remains as to how the mass is distributed. Because of the emission lines, UV continuum and IR excesses, the presence of a circumstellar shell seems likely. This shell is energized by a stellar core. The whole structure is complicated though, by rotation, mass loss and mass infall discussed below.

2. Dynamics

The spectrum indicates mass movement and the rapid changes in brightness seem to confirm that the T Tauri structure must be a dynamic one, though it is by no means clear whether dynamics of the envelope or of the photosphere are responsible.

a. Rotation

Analysis of the broadened photospheric absorption lines [Herbig, 1957] indicates rotation of the star. In comparison with other late main sequence stars, the T Tauri stars have substantially larger angular velocities [Rydgren, Strom, and Strom, 1975]. These velocities range from 20 to 100 km/sec. It is possible that the broadening is enhanced by the expanding circumstellar envelope [Strom, Strom, and Grasdalen, 1975].

b. Mass Loss and Infall

The evidence regarding radial motion of the T Tauri stars' mass sometimes seems contradictory. Most of the T Tauri stars show the P Cygni profile. This indicates an outflow of mass. This loss of mass seems to be one in which the mass totally escapes the star. It has been estimated to be as great as $3.7 \times 10^{-}$ solar masses per year [Kuhi, 1964].

Since T Tauri stars are supposedly young, newly contracted stars, this mass loss can be disquieting. It is believed that the mass escapes because there has not been observational evidence of any of the ejected matter returning. Prentice [1973] has suggested that the observed mass ejection is a convective overshoot from the photosphere; but the mass is slowed and the infall of material at about 10 km/sec would be undetectable against the normal motions of the atmosphere. It is believed by some that mass loss is a major process in even very young stars [Rydgren, Strom, and Strom, 1975].

As mentioned previously, some stars have been observed with inverse P Cygni profiles, indicating a rapid infall of material [Walker, 1972]. However, other interpretations regarding the intensity of various emissions are possible [Strom, Strom, and Grasdalen, 1975]. The weight of evidence supports mass ejection for most T Tauri stars; and while some infall is possible, it is probably not part of the stellar contraction or accretion processes as has been suggested [Rydgren, Strom, and Strom, 1975]. One would expect to observe spectroscopic evidence of stronger and more frequent infall in this group of stars, if they were truly in an accretion phase. In other words, occasional inverse P Cygni profiles alone cannot be viewed as spectroscopic confirmation of an accretion phase.

The mechanics of mass loss remain a mystery. It appears that the youngest stars have the greatest mass-loss rates [Rydgren, Strom, and Strom, 1975]. If emission line intensity can be correlated to mass-loss, then the observed fact, that emission line intensity tends to become less for older groups of T Tauri stars [Cohen, 1974], may be an important clue for a model. Just how the mass moves in connection with the contraction and how rotation is connected is unknown.

3. Lithium Abundance

Herbig [1962] reviews the work in the field of the lithium abundance in the T Tauri stars' composition. The abundance is about two orders of magnitude greater than the sun.

In stars with hydrogen burning lithium is destroyed rapidly. If T Tauri stars are indeed PMS objects, then the Galactic abundance of lithium may be indicated. However, schemes for the nucleosynthesis of lithium have been suggested. The actual cause of this high abundance is unknown.

C. PRE-MAIN SEQUENCE (PMS) STELLAR EVOLUTION

Since it is now generally accepted that the T Tauri phenomenon is a stage of stellar evolution through which at least some and possibly all stars pass, it is instructive to discuss that portion of a star's life prior to the stage when it begins its equilibrium hydrogen core burning, the main sequence, and to discuss how T Tauri stars can be assigned to the PMS set as support for a theory of stellar evolution.

1. Birth of a Star

There are regions of the galaxy, observationally close to earth, in which molecular hydrogen and dust (only about 1% of the interstellar medium) have a density great enough that radiation from more distant stars is completely obscured. These clouds are pierced by lines of magnetic flux and molded by large scale gravitational instabilities. They are bombarded by high energy cosmic rays and accelerated by various Alfvén waves in complicated schemes of coupling and decoupling. In a set of conditions, not well understood, in these clouds pockets of higher density may be formed. If the internal energy is not too great, the self-gravitation of the gas and dust may be great enough to accelerate the

matter towards a center of mass. This is the start of a collapse. By the Virial Theorm half the potential energy released in the collapse goes into internal heating of the system, and the rest must be radiated from the system. If the mass is great enough and the opacity of the cloud material is such that excess energy can be radiated away, then the gravitational forces can overceme thermal motions which would dissociate the dense pocket, and further accretion of the surrounding cloud can continue. Once there is a gravitationally bound system, a condition of dynamic hydrostatic equilibrium exists; and it is possible to model the system mathematically. This set of first order differential equations relate the pressure, mass, density, luminosity and temperature as functions of a radial distance from the center of mass. With knowledge or assumption about the local thermodynamic state, solutions can be found. Usually these solutions are carried out in terms of mass rather than radius and solved numerically. If one carries out a series of such calculations for a particular total stellar mass, then a complete history of the star's collapse, life and eventual death can be calculated. This history can be plotted on the H-R diagram, showing the sequence of luminosities versus effective surface temperatures. Such a history is called a track. Age is a parameter along such a track.

There are two distinct tracks currently accepted as possibilities for the PMS history. Both sets of calculations require the simplifying assumptions of no rotation, no

associated magnetic field and a spherical fluid, non-turbulent mass. The earlier set of calculations led to what are called the Hayashi tracks. These tracks require the additional simplifying assumptions of a roughly homologous collapse and a polytropic density distribution. Further, no provision is made for mass loss. More strenuous calculations yield the Larson tracks. These different tracks are discussed below; however, only the PMS tracks are discussed, not the main sequence and post-main sequence evolution. Regardless of model, the tracks differ greatly depending on the initial mass and the initial composition, so only a general comparison can be undertaken here, using a star of about a solar mass to compare the two tracks.

2. The Hayashi Track

A major result of Hayashi-type calculations is the establishment of a forbidden region. This is an area in the H-R diagram in which no stellar object in hydrostatic equilibrium can exist, because at any given mass and given luminosity, hydrostatic equilibrium is not possible if the surface temperature of the object is too cool [Clayton, 1968].

In the Hayashi scheme, as explained by Clayton [1968], the dense collapsing pocket starts almost in a free fall. Eventually temperature and pressure rise, slowing the collapse to a quasistatic state, one in which the partition of lost potential energy, half to kinetic (thermal) energy of the particles and half to radiation production, becomes a quite accurate description. Although the radiation escapes

easily at first, eventually there is increasing opacity. This is because opacity is a state function, determined by the changing density and temperature. While there is some additional heating because of this, interior temperatures cannot rise above about 10^4 °K until the molecular hydrogen has disassociated and ionized. When the ionization is complete there can be further contraction and heating until a state of dynamic hydrostatic equilibrium exists, in the homologous collapsing sphere.

It is at this point that the Hayashi track begins. A Hayashi track is shown in Figure 28. As was previously stated, since the surface temperature cannot be too cool, the star's appearance must take place at the near vertical boundary of the forbidden region in the H-R diagram. The surface temperature is high and contraction is still in progress, and the radius is large. This must result in a large luminosity. For a star of one solar mass, its starting luminosity is about 16 $L_\odot$ and effective temperature about 3900°K. The 3900°K is the coordinate of the boundary of the one solar mass forbidden region. In the Hayashi scheme, no star of one solar mass (with the same composition) can be cooler.

But the star is still gravitationally unstable and collapsing, a process which continues for about 10^6 years. With the calculated high opacity, the star must be fully convective to transmit radiation at the required rate to maintain quasistatic hydrostatic equilibrium.

Subsequent calculations show the star "moving" nearly vertically down the edge of the forbidden region on a track of only slightly increasing surface temperature but with a dramatic decrease in luminosity. But the resulting contraction increases central temperature and changes the central opacity. The evolution slows and a core in radiative equilibrium grows. Eventually nearly the entire star is in radiative equilibrium and the main sequence size is reached, but by now the central temperature and density is great enough for thermonuclear reactions to occur, supplying radiant energy at the same rate it is lost at the surface. At this time the star is positioned on the main sequence. During these final stages in which radiative transfer overcomes the convective phase, the decreasing luminosity ceases and the surface temperature increases. (There is a small increase in luminosity but the track is essentially horizontal.) Since a one solar mass star was picked, its surface effective temperature is about 5770°K with an absolute bolometric magnitude of $+4^{m}.75$.

For stars of greater mass, the forbidden region has its border at slightly greater temperatures and the convective phase takes a progressively smaller portion of the evolutionary time, until for stars of the greatest observed masses ($\geq 15\, M_{\odot}$), there is essentially no convective phase at all. In these cases the stars move on a track of increasing temperature with about equal luminosity.

3. The Larson Track

The Larson calculation does not take the Hayashi assumption of a homologous contraction nor the ensuing polytropic density distribution; but the assumptions of spherical symmetry, no rotation, no magnetic fields and negligible internal turbulent motions are retained. For further detail, the reader should consult Larson [1969 and 1972], and the review articles [Strom and Strom, 1973] and [Larson, 1973]. These sources were used for this summary.

The Larson scheme starts essentially like the Hayashi with a cloud collapsing in free fall, but not homologously. The interior density increases at the expense of the outer portions whose density decreases. Collapse in the outer regions is "significantly retarded from a free fall." This non-homologous collapse results in a peaked density distribution, the greatest density at the center. But furthermore, the collapse becomes most rapid at the center too. The result is major changes in density in a decreasing region about the center while little happens in the outer regions. Eventually, the central region becomes opaque and, with the rapidly increasing central pressure and temperature, the collapse is slowed and finally stopped. This core, in which collapse has ceased, is in sharp physical contrast with an intermediate region in which the molecular hydrogen continues to free fall. This abrupt change results in a shock front. Infalling material results in continued core collapse subsequent to a series of unimportant

rebound oscillations. Interestingly, the shock front which bounds the core moves with the core surface inward toward the center, even though it bounds increasing mass. Now, in this first core a second core is developed in just the same way except the molecular hydrogen is dissociated in the process, and this core is in hydrostatic equilibrium. A second shock front is formed but within the first core and the first shock front.

A rather complicated thermodynamic condition now exists at the second shock front, the result being an increase in the radius of the second core. The first shock front dies away as the expansion takes place.

Infalling of matter continues at the shock front, but there is a point when the opacity of this gas and dust drops so that radiant energy can be transported to the outside, eventually escaping into interstellar space. The result to an outside observer would be a rapid increase from almost no luminosity to about 10 times the luminosity of the sun. This is the start of the Larson track for the luminous object. A Larson track is shown in Figure 29. Were the core visible, it would have a radius about 12 solar radii and an effective temperature of about 3200°K for a single solar mass object. But this is within the Hayashi forbidden region, and part of the subsequent evolution will carry the star to even lower effective temperatures!

To review thus far, the Larson calculation results in the formation of a small stellar core which expands while

accreting additional material; whereas, in the Hayashi model there was a homologous overall contraction of a single cloud.

Because of the energy loss, the core begins to contract, and a convection zone starts at the core's surface, growing inward. Core contraction speeds up, fed by both radiative and convective energy losses. The smaller radius results in a lower luminosity. But the infall of material continues and the further evolution guides the track to greater luminosities and greater surface temperatures, even though in this phase the radius remains about constant. In this phase, there is a significant increase in the core mass, and the track moves out of the forbidden region. When about half the total cloud mass available is in the core, the final parts of the track and movement to the main sequence is started. At this point, the maximum effective surface temperature has been reached, about 8300°K, and the maximum luminosity, about 30 times that of the sun. As the remainder of the cloud mass accretes, the core, seeking a resultant static equilibrium state, moves back to a lower temperature and smaller luminosity. As the outside mass is depleted, the kinetic energy of the infalling material at the shock front is no longer a contributing luminosity source. There is, at this point, little infalling material, but there is convective transport in the outer half of the core. What exists, then, is a stellar object at the edge of the forbidden region with a central radiative core and a convective outer core, the whole object in final collapse.

It is, in fact, on the lower part of its Hayashi track but with a much smaller radius and luminosity than was predicted in the Hayashi scheme. It did not reach that point, however, in the same manner as the original Hayashi track. From this point the star follows the Hayashi track to the main sequence. In the case of protostellar clouds of two stellar masses and greater, the Larson calculations show that no convective Hayashi phase is reached at all.

The importance of the Larson scheme lies in its prediction of a non-homologous collapse resulting in a stellar core with a surrounding, infalling circumstellar cloud.

4. The Evolutionary State of T Tauri Stars

The question remains to be answered: just where do T Tauri stars fit onto an evolutionary track? The observational clues are: a stellar object with visible and infrared radiation (in excess), association with nebulosity and in some cases known young O and B stars, circumstellar envelopes with emission and blue continuum, large rotational velocities, and mass ejection and/or inflow. Additionally, the luminosity and temperature can be found for a few representative stars. These coordinates plot above the main sequence. Unfortunately, their masses are not known.

There appear to be two main positions on the question of the T Tauri stars' evolutionary state. The one delineated by Rydgren, Strom, and Strom [1975] takes exception to the explanation given by Larson [1972].

Larson [1972] argues that the T Tauri stars are probably "newly formed stars," this name being given to the protostar when it reaches the end of that portion of the Larson track beginning with the maximum temperature and luminosity (half the mass in the core) and ending just at the start of the Hayashi convection phase (nearly all the mass in the core), recognizing that for $M \geq 2M_{\odot}$ there is no Hayashi convection phase. Larson points out that the predicted locus of "newly formed stars" lies near, but below, the isochrone for 10^6 years. Larson's explanation might fit some of the evidence, except the plotted H-R positions and the lack of observed inverse P Cygni profiles.

This last fact is the crux of Rydgren, Strom, and Strom's [1975] disagreement. The T Tauri stars (a Taurus-Auriga group and a ρ Ophiuchus group), which they have plotted, fall substantially above the 10^6 year isochrone. Further, they argue that optically thick circumstellar dust shells are rare among the T Tauri stars, and thirdly, they point out that the inverse P Cygni profile is observed in only one of their sample stars and that star has the lowest luminosity of the group. They conclude that there is no "final accretion phase" and that the T Tauri stars are actually on radiative equilibrium tracks approaching the main sequence.

While Rydgren, Strom, and Strom may be correct, their arguments do not necessarily refute Larson's thesis. First, the masses are not well known, so comparison of their

locus with Larson's locus drawn for specified masses is hardly conclusive. Furthermore, the two groups of Rydgren, Strom, and Strom have about the same locus, yet the ρ Oph group is known to be older. Second, Larson's locus would change if rotational effects were included. This is a particularly important point since the angular velocities for T Tauri stars seem to be high. The effect of rotation might very well move the Larson locus above the 10^6 year isochrome. Third, there is no requirement in the Larson track for an optically thick circumstellar shell at the time the "newly formed stars" appear; rather, if the star is appearing (visually) the shell must be becoming optically thin. Fourth, while it is true that the P Cygni profile is observed with far more frequency than the inverse profile, the evidence is not conclusive that mass is ejected permanently. A slow unobservable infall is possible, as was previously mentioned. In any case, at the point where Larson's "newly formed stars" appear there is no further requirement for mass infall since "practically all of the proto-stellar mass has fallen into the core" [Larson, 1969]. Furthermore, the mass loss may not be isotropic. However, some explanation for mass ejection is still needed.

III. PRESENTATION OF DATA

For this research the data for the 323 stars listed in the Catalog required reduction and coding to make computer processing possible. Where qualitative labels were given in the Catalog, numerical values were assigned. Data processing and some of the statistical analyses were accomplished using the Naval Postgraduate School IBM 360-67 computer system. The library programs of the Statistical Package for the Social Sciences (SPSS), revision V [Nie, Bent, Hull, 1970] were used for the majority of this work. Additional regression analyses were made with a program provided by Mr. Robert Batesole of BDM Corporation that allowed for a search of the best of all possible regressions, and the regression analysis routines of Biomedical Computer Programs (BMD) library.

Notwithstanding its name, SPSS provided an excellent tool for this project. It allowed versatile data selection, recoding and labeling. Further, its graphics were easy to generate and understand.

In the paragraphs that follow, a broad look at the Catalog's data will first be given, followed by closer looks at specific relationships. No attempt was made to look at every possible relationship between variables. Some were clearly not related and others had so few cases with complete data that analysis was not significant. Missing values were not

allowed to affect statistics. In addition to the characteristics of the Catalog, two additional variables were added: MASPRD, which was calculated from the difference between brightest and dimmest apparent magnitudes (m (MAX) - m (MIN)); and AMPG, the absolute photographic magnitude (M_{pg}), which was calculated from distances and absorptions of prior research.

One additional amplifying note needs to be made. The Catalog's stars were divided into four rough groups (subfiles) by presumed physical association as given in the Catalog. The four subfiles used were defined as follows:

(1) ORION subfile--86 stars identified with the Orion Nebula.

(2) TAUAUR subfile--58 stars identified with the Taurus-Auriga region.

(3) NGC2264 subfile--34 stars identified with NGC2264.

(4) OTHERS subfile--All those stars not a member of the other three subfiles. This subfile includes stars which are identified with specific New General Catalog (NGC) or Barnard designations even though they may be close to the Orion nebula or Taurus-Auriga region. There are 145 stars in the OTHERS subfile.

Except where otherwise noted, all stars are considered in the discussions below. Cases with missing data are excluded only in the considerations of the particular variable with missing data.

A. BROAD LOOK AT CHARACTERISTICS

1. Position in Galactic Coordinates

The Catalog gives the galactic coordinates expressed in the 1958 system [Allen, 1973]. The variable names GALONG

and GALAT correspond to ℓ^{II} and b^{II} respectively, now more usually labeled ℓ and b.[2]

The range of ℓ is the full 360° while b has values from -34° to +23.3°. Now, referring to Figure 1, it is interesting to note that all three of the major concentrations of Catalog stars (ORION, TAUAUR and NGC2264) lie in the region $155° < b < 215°$, a rather narrow band. Interestingly, this band of high concentration is bounded on each side by bands of no Catalog stars at all. This presumedly involves the structure of a nearby Galactic spiral arm.

The mean value of b is -8.7°. Excluding the ORION subfile the mean is -5.0°. Only after excluding TAUAUR subfile does b move within two degrees of the Galactic plane at 1.5°. Again, this is an indicator of local Galactic structure.

Histograms of the two Galactic coordinates are given in Figures 2 and 3.

2. Apparent Magnitudes

Photographic apparent magnitudes (m_{pg}) are given for 278 stars (86.1% of the total number of Catalog stars). No attempt was made to calculate corrections for the 45 stars whose magnitudes were given at a visual wavelength.

---

[2] The Galactic center ($\ell = 0$, $b = 0$) is in the direction of the constellation Sagittarius at right ascension $17^h\ 39^m.3$ and declination -28° 54' (1900). In general, the value of ℓ (GALONG) indicates the direction towards or away from the Galactic center while b (GALAT) indicates a measure of distance above or below the galactic plane.

The 278 stars with photographic magnitudes have the following characteristics:

	BRTMAG	DIMMAG
mean	$13^{m}.7$	$15^{m}.5$
std. dev.	1.8	1.6
max	$18^{m}.0$	$18^{m}.0$
min	$7^{m}.2$	$8^{m}.0$

Dimmest magnitudes were not given for 118 stars (36.5%). Where only one magnitude was given, it was taken to be the brightest.

Histograms of BRTMAG and DIMMAG are shown in Figures 4 and 5 for all stars and thus include the visual magnitudes. The histograms are shown for interest only and the error introduced by the visual magnitudes is small.

3. Range of Apparent Magnitudes

The range of apparent magnitudes was calculated by taking the absolute difference between BRTMAG and DIMMAG. There were 205 stars (63.5%) for which such a range could be calculated. The following statistics were calculated for MASPRD:

mean	2.07
std. dev.	1.1
max	6.8
min	0.2

The histogram is shown in Figure 6.

Considering only the certain and presumed T Tauri stars, a mean MASPRD of 1.89 was found, lower but not significantly so. In calculating MASPRD, no correction was made for the difference in magnitude systems; that is, the difference in visual magnitudes was considered to be a comparable indicator to that of photographic magnitudes.

4. Light Curves

Only 141 stars had an assigned light curve classification. Of these 20 had anomalous classifications. The remaining 121 stars are divided among the classes as follows:

more frequently bright than faint.....30 stars (9.3%)
most frequently has the mean brightness..35 stars (10.8%)
more frequently faint than bright.....31 stars (9.6%)
no preference at any level.....25 stars (7.7%)

5. The statistics for the photometry are given in Table II. The histograms of V, B-V and U-B are shown in Figures 7, 8 and 9 respectively.

6. Spectra

Spectral types of Orion Population stars range from a hot B5 ($T_e = 15,500°K$) to a cool M5 ($T_e = 2800°K$). Seventeen stars have no classification at all, 14 stars have vague classifications (e.g., G-K), 97 stars appear to have continuous spectra, and 20 stars show clearly continuous spectra. While the stars that appear to have continuous spectra may have some underlying structure, it remains generally not resolved. A histogram of the rough spectral classifications

appears in Figure 10. This histogram is for all the stars in the Orion Population.

Considering only certain T Tauri or probable T Tauri stars, the distribution is like the one for all stars. There is only one star (V380 Ori) earlier than F5 and its spectrum is slightly uncertain, although its position as main sequence dwarf is assumed. As can be seen in Figure 11, the numbers in each rough spectral class increase towards the later types with a maximum number of 16 in spectral class K5. While only 14 stars have some sort of M type spectra, it has been pointed out that this decrease in numbers is probably an observational limit brought about by the low visual magnitudes of these faint objects [Herbig, 1962]. Stars earlier than middle F are not classed as T Tauri stars, since the specific criteria of variability and the usual quality of noticeable line broadening (rotation) are not apparent in earlier types [Walker, 1956]. Those early (Be and Ae) stars not fitting the T Tauri criteria are known as Herbig Emission stars. They are similar in their emission characteristics and association with nebulosity. Why the high rotation and irregular variability should start at middle F and extend through all the later stars is not known. The lesser mass probably has some effect on the dynamics of stellar evolution beyond the schemes of Hayashi and Larson.

For the sake of completeness, a summary of the other spectral information must be pointed out. Two stars, FU Ori and CPD-76°652, have supergiant luminosity classes. Six stars

have, or are close to, giant luminosity classes and one star, AN Ori, has a clear luminosity class of IV. There are 41 stars with dwarf luminosity classes; but for 273 stars (84.5%) of the Orion Population the luminosity class cannot be determined because the luminosity criteria in the spectra are missing.

7. Emission Line Intensity

The emission line intensity is a set of qualitative categories by which the existence, development and intensity of a star's emission relative to the continuum can be defined. This system was set up by Herbig [1962]. The emission line intensity is not constant, the lines are more intense when the star is brighter. The Catalog only gives one emission intensity and does not indicate at what point in the light curve the spectrum was taken. It might be assumed that the Catalog is slightly weighted towards stars with brighter emission line intensities since these stars are more likely to have been discovered.

The code assignment increases with increasing emission intensity, proceeding from no emission lines to the advanced T Tauri-type spectrum. A histogram of the emission intensities is shown in Figure 12.

Cohen [1974] has described how younger clusters tend to have distributions such that there is a greater number proportionally of T Tauri stars having greater emission intensities. In older clusters the number densities tend to favor lesser categories of emission intensities.

Cohen's results were checked using the much larger sample size of this study to plot the histograms and calculate chi-squared statistics for testing his hypotheses. Cohen's results are supported.

8. Types of Stars in the Catalog

Given below is the number of stars assigned to each rough specification of the star's type:

no information	114
certain T Tauri	127
presumed T Tauri	32
hot member (usually of spectral class B or A)	21
a late type star of low to moderate luminosity	20
peculiar object	9

B. ABSOLUTE MAGNITUDES

On the basis of thorough literature research for distances, reddening and absorption, absolute photographic magnitudes were calculated for 228 stars. The distance moduli, $(m_{pg} - M_{pg})$, and absolute photographic magnitudes (M_{pg}) are listed in Table III along with the source.

1. Calculation of Distance Modulus

In general, a distance and monochromatic extinction in magnitudes is required to calculate a distance modulus, $(m - M)$, from the well known relationship

$$(m - M) = 5 \log(d) - 5 + A$$

where: m is the apparent magnitude:

$$m = \text{constant} - 2.5 \log F$$
$$= \text{constant} - 2.5 \log \left(\frac{L}{4\pi d^2}\right)$$
$$= \text{constant} + 5 \log d - 2.5 \log L ;$$

and where: d is the distance from earth to the star, usually in parsecs (pc), F is the monochromatic flux, L is the monochromatic luminosity, and A is an absorption in magnitudes;
and where: M is the absolute magnitude which is defined as the apparent magnitude of a star at a standard distance of 10 pc, that is

$$M = \text{constant} + 5 - 2.5 \log L .$$

2. Calculation of Absorption

The value of the absorption is rather more complicated to calculate because a star's light is not only dimmed but reddened. Because longer wavelengths are not absorbed to the same extent as shorter wavelengths it is possible to calculate a ratio (R) of total to selective absorption when photometry and an intrinsic (unreddened) color can be found. It is unfortunate that this ratio is not everywhere constant. Newly calculated values were used wherever available; but when R was unknown the standard value $R \simeq 3$ was used. With a value of R, the absorption A was calculated from

$$A = R \times E,$$

where E is the color excess, that is, the difference between the observed and intrinsic colors. Colors are defined as the difference in magnitude between apparent magnitudes, which are observed at two different effective wavelengths, for example, B - V.

For those stars for which no value of R or E could be found, a standard absorption was assumed depending on the stars' galactic latitude.

3. Calculation from Luminosity

In a few cases absolute magnitudes were determined directly from the total luminosity using the below relationship and bolometric corrections from Allen [1973].

$$M_{bol} = 4.75 - 2.5 \log L \text{ (in solar units)}.$$

4. Results of Calculations

The formulae above were used whenever the data permitted. Special assumptions regarding the calculations are contained in the Notes to Table III. Except where noted, all magnitudes were corrected to photographic magnitudes. A histogram of the absolute magnitudes is shown in Figure 13. The distribution of stars in M_{pg} by subfile groups is discussed in a later section on the luminosity function. The following statistics were calculated for M_{pg}:

mean	$4^{m}.8$
std. dev.	$2^{m}.1$
max	8.8
min	-4.1

C. RELATIONSHIPS BETWEEN CHARACTERISTICS

There are many cross relationships that can be formed between various categories given in the Catalog. Many of these were studied using Cartesian scatterplots and two-way frequency tables. Where indicated, second order effects

were examined. Individual H-R diagrams, using apparent magnitudes, for Taurus-Auriga, Orion and NGC2264 were examined; but differential reddening and extinction badly scattered the results, and so the diagrams were not helpful. This problem may still be a factor even in H-R plots using M_{pg} since for ORION and NGC2264 an average extinction was used throughout, a clear probable error of up to a magnitude, at least in the ORION subfile. For the few stars with a characteristic period, no relationship was found between the characteristic period and the star's absolute magnitude.

Three sets of relationships of particular interest are discussed below.

1. Correlation with the Range of Apparent Magnitudes with Other Characteristics

When this research began, it was assumed that the range in apparent magnitude (MASPRD) was related to the dynamics of the star in some way; and that being so, a correlation would be found between MASPRD and some other observable characteristic. In a thorough analysis, no significant correlation between MASPRD and any other variable or set of variables could be found.

MASPRD was plotted on two-dimensional scatterplots against each of the following variables without significant correlation: GALONG, GALAT, BRTMAG, DIMMAG, V, BMNSV, UMNSB, TEMP, EMINT, and AMPG. The highest correlation was with BRTMAG ($r = 0.4$). A two-way frequency distribution was

prepared for MASPRD and LICRV. There was no essential difference in the distribution of MASPRD for the four main light curve classes. For the variable TEMP only those stars with well defined non-continuous spectra were considered, since stars with continuous spectra were given identical codes. Thus there was no correlation between MASPRD and the effective photospheric temperature.

There were 61 stars that had values of BRTMAG, DIMMAG, V, BMNSV, TEMP, EMINT for all cases. A program was prepared to find the best of all possible regressions of these variables with MASPRD as the dependent variable. A linear combination of BRTMAG and V provided the best correlation; however, the calculation of an F statistic confirmed the poorness of fit. A stepwise regression was also run with similar results. A plot of the residuals versus the variables showed no underlying structure. Factor analysis was not undertaken, but may show some significant tie undiscovered in the regression analysis. This possibility is considered unlikely. At this time, there is no clear relationship between the spread in apparent magnitudes and any other observable characteristic or set thereof.

This is particularly disturbing in the case of the lack of any relationship between MASPRD and the emission intensity (EMINT), a scatterplot of which is shown in Fig. 14. There are many indications that the emission intensity and variability are related. As stated previously, the emission lines are stronger when the star is at maximum light.

Some strong emission line stars show small light variations on a short time scale in addition to the large variations characterized by MASPRD, while weak emission line stars do not show the small variations [Rydgren, Strom, and Strom, 1975]. It has been asserted by Rydgren, Strom, and Strom [1975] that "the principal source of variability in T Tauri stars is the changing strength of the envelope emission." Lastly, those characteristics which delineate PMS objects should lessen in degree and disappear as the star evolves to the main sequence.

Since main sequence stars have neither irregular variability nor emission lines, and the PMS T Tauri stars do, presumedly both emission strength and variability decrease in, at least, a qualitative way with increasing stellar age. But Figure 14 shows no tendency for MASPRD to change with EMINT. Statistical tests confirm the visual observation that there is no correlation. No current theories explain either the cause of the irregular variability, nor why MASPRD should be independent of the other observed characteristics.

The question of the correlation between the magnitude of the variability and the emission intensity may be important to determining the true nature of certain A and F stars. Strom, Strom, and Grasdalen [1975] have suggested that if the variability and envelope emission strength are correlated, then certain weak Hα stars may be small amplitude variables. No correlation can be suggested on the basis of this research.

2. Hertzsprung-Russell Diagrams

The poor results obtained from plotting apparent magnitudes versus either the spectral class or the color B - V have already been discussed. The use of the absolute magnitude improves these plots considerably, particularly in the H-R diagram of the Taurus-Auriga region. The list below shows some of the H-R diagrams plotted in this research:

Figure 15 - M_{pg} vs. TEMP - all stars

Figure 16 - M_{pg} vs. TEMP - subfile OTHERS

Figure 17 - M_{pg} vs. TEMP - subfile TAUAUR

Figure 18 - M_{pg} vs. TEMP - subfile NGC2264

Figure 19 - M_{pg} vs. TEMP - subfile ORION

Figure 20 - M_{pg} vs. TEMP - all certain or probable T Tauri stars

Figure 21 - M_{pg} vs. B - V - all stars

Figure 22 - M_{pg} vs. B - V - subfile OTHERS

Figure 23 - M_{pg} vs. B - V - subfile TAUAUR

Figure 24 - M_{pg} vs. B - V - subfile NGC2264

Figure 25 - M_{pg} vs. B - V - subfile ORION

Figure 26 - M_{pg} vs. B - V - all certain or probable T Tauri stars

The dwarf main sequence is drawn on each.

Two items regarding these diagrams are causes of error. First, most of the stars (ORION and NGC2264) had their absolute magnitudes calculated on the basis of an average extinction. This could cause an estimated standard error of as much as 1 magnitude. However, since the error

is applied to stars equally in both directions, the overall effect probably does not bias the considerations of large scale characteristics from the H-R diagrams. On the other hand, the absolute magnitudes for the Taurus-Auriga stars have quite small standard errors, probably no greater than ±0.3 magnitudes. This is because much closer estimates of individual extinction could be applied, given the excellent photometry and calculations of Rydgren, Strom, and Strom [1975]. Second, but for equivalent reasons, the H-R diagrams with B-V as the abscissa are in even greater error, because not only are the M_{pg}'s in error as above; but the reddening is variable also. Consequently, a star's horizontal position is not only offset to a greater B-V because of overall reddening, but is uncertain by an amount not determined. Again, for recognition of gross characteristics these errors are probably inconsequential.

After examination of the diagrams there can be little doubt that Orion Population stars usually have luminosities greater than main sequence stars of the same spectral class, at least for mid-F stars and later. There are seven stars earlier than F5 with peculiar luminosities. Particularly strange are LkHα 198 (HRC 3) and LHα 25 (HRC 219). These stars are too dim by about three magnitudes. LHα 25 is in NGC2264, a cluster with a well determined distance modulus [Walker, 1956]. Its spectrum, B8pe + shell, indicates a source of circumstellar extinction. The most probable cause of the error is a large difference in the extinction from

the average value assumed for NGC2264. The distance modulus for the small anonymous dark nebula close to LkHα 198 has been determined spectroscopically from two main sequence B stars [Herbig, 1960]. LkHα 198's spectrum is an uncertain A and so the necessary absorption to take the star to the main sequence ranges from two to four magnitudes. Extinction is probably the cause of the anomaly, but too little is known about this nebula to draw any firm conclusions. The other five stars may truly be large mass PMS objects or the absorption has been badly overestimated.

For the F5 and later stars the H-R diagrams combined with the various spectral peculiarities would seem to confirm their PMS nature. On the basis of these H-R diagrams alone, particular "tracks" cannot be chosen. But from Figure 15 one can see that the cross section of Catalog stars covers stages of evolution from early visual appearance to positioning on the main sequence, if Larson tracks are assumed.

3. The Relationship Between the Light Curve Classification and the Emission Intensity

It has been previously shown that there is no correlation between EMINT and MASPRD and further, that the distribution of MASPRD does not change between the various light curve classifications. It seems reasonable that if EMINT and MASPRD are independent and if the distribution of MASPRD for each LICRV class is the same (and possibly random), that there might be some information gained by considering a two-way frequency table of LICRV and EMINT. This cross

tabulation is shown in Table IV. In making this table, intermediate categories of EMINT, that is, EMINT = 1.5, 2.5, 3.5 or 4.5, were counted as the next highest value. For example, cases with EMINT = 1.5 are counted as cases with EMINT = 2.0. A chi-squared statistic was calculated to test the hypotheis that the distributions of EMINT between light curve classifications were equivalent. The distributions of EMINT differ at a 99% confidence level. This may clearly be seen by examination of Table IV, row by row. The interesting effect is that those stars which are more frequently bright than faint have clearly the weakest emission intensity. Recall that for individual stars, emission line strengths are greatest when the stars are brightest. Furthermore, this difference is still distinct if a statistical collapse is made with intermediate categories moved to the next lower value or even split between values. The light curve classification with the strongest emission intensity is the group which most frequently has the mean brightness. No simple explanation is apparent.

D. THE LUMINOSITY FUNCTION

The luminosity function shows the relative numbers of stars in successive intervals of absolute magnitude for a given volume of space. In Figure 27 the histograms of M_{pg} for each of the three specific subfiles and for the luminosity function [Allen, 1973] are shown. The luminosity function (M_{pg}) gives the number of stars per unit volume within the magnitude range M - 1/2 to M + 1/2. The sharp

divergence between the observed results and the luminosity function at about $M_{pg} = +6$ is probably due in part to observational selection. The faint-end cut-off, however, appears to be too sharp to be explained by observational limitations alone; thus the luminosity function for T Tauri stars appears to be significantly different than the luminosity function for the solar neighborhood. This difference is not predicted by theory.

IV. CONCLUSIONS

The major results of this research were estimates of absolute magnitude for 228 Orion Population stars, the calculation of a variety of statistics for the Catalog's categories, the production of frequency distributions, and the creation and statistical testing of many cross relationships between the Catalog's variables. This included Hertzsprung-Russell diagrams. These H-R diagrams are quite accurate particularly in the Taurus-Auriga region. There is no Orion Population star F5 or later with an anomalous position.

The Orion Population stars, of which T Tauri stars are a major subset, are largely pre-main sequence objects evolving towards the main sequence. All current theories of stellar evolution predict the appearance of stars with H-R diagram positions that the T Tauri stars have been observed to fill. The majority of the plotted stars fall well below the giant star branch. However, on the basis of large scale considerations of the Catalog data, no conclusive argument can be made for any particular track, convective or radiative.

One could certainly reach this conclusion only on the basis of a lack of understanding of the hydrodynamics. The theories of Larson and Hayashi do not explain the mass loss, variability, or our results. On the basis of this work there does not seem to be any connection between the large

scale variability as represented by MASPRD and any other observable characteristic. Since one expects the directly observable characteristics to be linked through the equations of hydrodynamic equilibrium, clearly the full dynamical situation cannot yet be understood. There does seem to be a relationship between the emission intensity and light curve classification, but this is also not yet explainable.

The sharp cut-off observed in the luminosity function indicates a population for T Tauri stars differing from the solar neighborhood. The cut-off appears in each of the major groups of T Tauri stars. It may be indicative of T Tauri structure as yet unexplained in theory.

TABLE I. CATEGORIES OF THE HERBIG-RAO CATALOG

	Category	Fortran Name
1.	HRC Number	HRC
2.	Indication of associated bright nebulosity	NEB
3.	Star name or other designation	none
4.	Right ascension and declination (1950)	none
5.	Galactic coordinates (1958) "ℓ"	GALONG
	"b"	GALAT
6.	Apparent magnitudes (m):	
	Brightest magnitude	BRTMAG
	Dimmest magnitude	DIMMAG
7.	Light curve classification	LICRV
8.	Comments regarding the light curve	LICOM
9.	Logarithm of a characteristic time interval in days, over which the star has been observed to undergo a major change in light and to recover	CRVLOG
10.	Mean visual photometric magnitude (V)	V
11.	Mean value of the color B-V	BMNSV
12.	Mean value of the color U-B	UMNSB
13.	Ultraviolet excess information	UVEX
14.	Uncertainty of photometric data	MUNC
15.	Comment regarding variations in V	IVARV
16.	Spectral class	TEMP
17.	Luminosity class	L
18.	Information of emission lines	IE
19.	Rough specification of the type of star	ITYPE
20.	A number describing the general intensity of the emission spectrum	EMINT
21.	Code indicating if Herbig examined spectrum plate	H
22.	Indication of abnormally strong ultraviolet continuum	IUCON
	Categories not in the Catalog but Used in this Project	
23.	The difference between the brightest apparent magnitude and the dimmest apparent magnitude, i.e., DIMMAG - BRTMAG	MASPRD
24.	The absolute photographic magnitude, M_{pg}	AMPG

TABLE II. PHOTOMETRY

Photometry of Orion Population

	V	B-V	U-B
Valid observations	137	134	120
Missing observations	186	189	203
Mean	$12^{m}.93$	$1^{m}.09$	$0^{m}.24$
Median	$13^{m}.26$	$1^{m}.12$	$0^{m}.23$
Std. dev.	1.9	0.4	0.6
Max.	$16^{m}.94$	$2^{m}.14$	$2^{m}.33$
Min.	$7^{m}.01$	$0^{m}.14$	$-1^{m}.32$

Photometry of Certain or Presumed T Tauri Stars

	V	B-V	U-B
Valid observations	72	72	65
Missing observations	87	87	94
Mean	$13^{m}.24$	$1^{m}.14$	$0^{m}.11$
Median	$13^{m}.48$	$1^{m}.16$	$0^{m}.05$
Std. dev.	1.6	0.3	0.6
Max.	$16^{m}.94$	$1^{m}.80$	$2^{m}.33$
Min.	$9^{m}.24$	$0^{m}.50$	$-1^{m}.32$

TABLE III. ABSOLUTE PHOTOGRAPHIC MAGNITUDES

HRC	STAR	LOCATION	$(m-M)_{pg}$	M_{pg}	REFERENCE	NOTE
1	MacC H12	CEP IV	12.8	4.4	1, 2	
2	Lk Hα 197	ADN	9.9	7.1	3	1
3	Lk Hα 198	ADN	9.9	5.1	3	
4	MacC H10	CEP IV	12.8	3.6	1, 2	
5	MacC H9	CEP IV	12.8	3.3	1, 2	
6	Lk Hα 200	NGC 225	10.2	3.8	1, 2	
7	Lk Hα 201	NGC 225	10.2	3.8	1, 2	
17	L Hα 92	IC 348,B4	9.2	7.3	4	
18	L Hα 97	IC 348,B4	9.2	8.8	4	
20	Lk Hα 330	IC 348	9.2	3.8	4	
40	Lk Hα 101	NGC 1579	13.9	3.1	5	
84	CO Ori	B 225	8.1	3.5	6	
85	GW Ori	B 225	8.1	2.6	6	
86	V649 Ori	B 225	8.1	4.9	6	
164	V380 Ori	NGC 1999	10.5	0.3	7	
183	V625 Ori	B 35	12.6	2.2	7	2
184	V630 Ori	B 35	12.6	2.5	7	2
185	V631 Ori	B 35	12.6	2.4	7	2
186	FU Ori	B 35	12.6	-2.4	7	
187	Lk Hα 314	NGC 2068	8.6	6.4	8	3
207	R Mon	NGC 2261	---	-2.7	7	
251	RU Lup	ADN	---	4.0	9	4
255	Do-Ar 9	B 42	9.6	3.4	10	5
256	Haro 1-1	Near B 42	8.9	5.5	10	

TABLE III (continued)

HRC	STAR	LOCATION	$(m-M)_{pg}$	M_{pg}	REFERENCE	NOTE
257	Haro 1-4	B 42	10.3	3.8	10	
258	V852 Oph	B 42	9.6	5.2	10	5
259	S-R 4	B 42	9.7	3.3	10	
260	Do-Ar 22	B 42	9.6	3.4	10	5
261	Haro 1-8	B 42	10.0	5.5	10	
262	S-R 24	B 42	9.6	5.4	10	5
263	S-R 12	B 42	9.6	3.9	10	5
264	S-R 9	B 42	8.9	3.6	10	
265	S-R 10	B 42	8.7	6.3	10	
266	V853 Oph	B 42,44	9.6	3.7	10	5
267	Haro 1-14	B 42	9.6	6.2	10	5
268	Haro 1-16	B 44	10.6	5.3	10	
277	Lk Hα 122	NGC 6514	12.2	3.8	4	
278	V1752 Sgr	NGC 6523	12.2	4.7	2	
279	Lk Hα 102	NGC 6523	12.2	2.8	2	
280	SV Sgr	NGC 6523	12.6	2.1	2	
281	Lk Hα 118	NGC 6523	12.2	-0.2	2	
288	R CrA	NGC 6729	13.1	-1.9	7	
290	T CrA	NGC 6729	10.2	2.2	7	
299	V521 Cyg	NGC 7000	14.7	0.8	7	6
300	V1057 Cyg	NGC 7000	14.7	-4.1	7	
301	Lk Hα 191	NGC 7000	14.7	-0.7	7	6
308	Lk Hα 349	IC 1396	12.7	2.3	4	
310	BD+46°3471	IC 5146	11.7	-1.3	1	
311	Lk Hα 245	IC 5146	11.7	4.9	1	

TABLE III (continued)

HRC	STAR	LOCATION	$(m-M)_{pg}$	M_{pg}	REFERENCE	NOTE
312	Lk Hα 257	IC 5146	11.7	2.1	1	
314	Lk Hα 350	Cep III	12.8	3.2	1	
319	MacC H3	Cep IV	12.8	2.7	1	7
320	MacC H3	Cep IV	12.8	3.1	1	7
321	Lk Hα 259	Cep IV	12.8	3.7	1	7
322	MacC H5	Cep IV	12.8	4.6	1	7
323	MacC H18	Cep IV	12.8	2.6	1	7
23	FM Tau	Tau-Aur, B209	9.9	4.8	10	8
24	FN Tau	Tau-Aur, B209	9.7	5.9	10	
25	CW Tau	Tau-Aur, B209	11.6	4.4	10	
26	FP Tau	Tau-Aur	6.4	8.6	10	
27	CX Tau	Tau-Aur	6.5	8.6	10	
28	CY Tau	Tau-Aur, B27	9.7	5.0	10	9
29	V410 Tau	Tau-Aur, B7	9.7	2.3	10	9
30	DD Tau	Tau-Aur, B10, B7	10.2	5.1	10	
31	CZ Tau	Tau-Aur, B10, B7	9.1	7.6	10	
32	BP Tau	Tau-Aur, near B7	7.9	4.9	10	
33	DE Tau	Tau-Aur	8.8	5.5	10	
34	RY Tau	Tau-Aur, B214	8.4	3.3	10	
35	T Tau	Tau-Aur	9.0	2.5	10	
36	DF Tau	Tau-Aur	9.0	3.5	10	10
37	DG Tau	Tau-Aur, B217	9.0	3.5	10	10

TABLE III (continued)

HRC	STAR	LOCATION	$(m-M)_{pg}$	M_{pg}	REFERENCE	NOTE
38	DH Tau	Tau-Aur, B19	7.3	7.7	10	11
39	DI Tau	Tau-Aur, B19	7.3	7.0	10	
41	IQ Tau	Tau-Aur, B218	9.0	6.3	10	10
43	UX Tau A	Tau-Aur	8.3	3.7	10	
44	FX Tau	Tau-Aur, B18	8.7	6.1	10	12
45	DK Tau	Tau-Aur, near B19	9.75	3.7	10	
46	ZZ Tau	Tau-Aur, B18	8.7	5.5	10	12
47	Lk Hα 331	Tau-Aur, B18	8.7	7.8	10	12
48	HK Tau	Tau-Aur, B18	8.7	7.6	10	12
49	HL Tau	Tau-Aur	13.8	1.2	10	12
50	XZ Tau	Tau-Aur	13.8	1.7	10	13
51	Lk Hα 266	Tau-Aur	10.0	5.0	10	
53	UZ Tau p	Tau-Aur, B19	9.0	5.0	10	10
54	GG Tau	Tau-Aur	9.0	4.7	10	
55	GH Tau	Tau-Aur, B18	8.7	6.0	10	12
56	GI Tau	Tau-Aur, B18	9.4	5.7	10	
57	GK Tau	Tau-Aur, B18	9.4	4.7	10	
58	DL Tau	Tau-Aur, near B18	10.0	4.5	10	
59	IS Tau	Tau-Aur, B19	9.0	7.5	10	10
60	HN Tau	Tau-Aur	10.8	3.7	10	
61	CI Tau	Tau-Aur	10.2	4.0	10	13

TABLE III (continued)

HRC	STAR	LOCATION	$(m-M)_{pg}$	M_{pg}	REFERENCE	NOTE
62	DM Tau	Tau-Aur	6.9	7.8	10	
63	AA Tau	Tau-Aur, B18	8.4	5.2	10	
64	HO Tau	Tau-Aur	8.8	7.4	10	13
65	DN Tau	Tau-Aur, B18	7.5	6.2	10	
66	HP Tau	Tau-Aur	8.8	7.2	10	13
67	DO Tau	Tau-Aur, B22	11.7	3.4	10	
68	VY Tau	Tau-Aur	7.5	5.8	10	13
69	Lk Hα 332	Tau-Aur, B22	10.2	6.3	10	13
70	DP Tau	Tau-Aur, B22	10.2	5.0	10	13
71	GO Tau	Tau-Aur, B22	10.2	5.9	10	13
72	DQ Tau	Tau-Aur	8.8	6.4	10	13
73	Haro 6-37	Tau-Aur	8.8	7.0	10	13
74	DR Tau	Tau-Aur	8.8	5.7	10	13
75	DS Tau	Tau-Aur	8.8	5.1	10	13
76	UY Aur	Tau-Aur	10.2	2.7	10	13
77	GM Aur	Tau-Aur	8.8	4.7	10	13
78	AB Aur	Tau-Aur	10.2	-2.5	10	13
79	SU Aur	Tau-Aur	5.9	3.4	10	
208	KV Mon	NGC 2264	9.85	6.1	11	
210	LL Mon	NGC 2264	9.85	6.6	11	
211	PT Mon	NGC 2264	9.85	7.6	11	
212	LM Mon	NGC 2264	9.85	6.9	11	
213	NW Mon	NGC 2264	9.85	5.7	11	

TABLE III (Continued)

HRC	STAR	LOCATION	$(m-M)_{pg}$	M_{pg}	REFERENCE	NOTE
214	LP Mon	NGC 2264	9.85	6.7	11	
215	LHα 21	NGC 2264	9.85	4.7	11	
216	NX Mon	NGC 2264	9.85	6.5	11	
217	W 84	NGC 2264	9.85	2.7	11	
218	LQ Mon	NGC 2264	9.85	7.4	11	
219	LHα 25	NGC 2264	9.85	3.3	11	
220	LR Mon	NGC 2264	9.85	5.2	11	
221	LT Mon	NGC 2264	9.85	5.9	11	
222	W 108	NGC 2264	9.85	2.5	11	
223	V419 Mon	NGC 2264	9.85	5.4	11	
224	V347 Mon	NGC 2264	9.85	7.6	11	
225	LU Mon	NGC 2264	9.85	6.2	11	
226	IO Mon	NGC 2264	9.85	4.9	11	
227	IP Mon	NGC 2264	9.85	4.6	11	
228	LY Mon	NGC 2264	9.85	6.5	11	
229	LX Mon	NGC 2264	9.85	5.7	11	
230	SS Mon	NGC 2264	9.85	4.7	11	
231	V360 Mon	NGC 2264	9.85	4.1	11	
232	V426 Mon	NGC 2264	9.85	4.8	11	
233	V363 Mon	NGC 2264	9.85	6.2	11	
234	MM Mon	NGC 2264	9.85	5.2	11	
235	LHα 61	NGC 2264	9.85	4.6	11	
236	V365 Mon	NGC 2264	9.85	5.7	11	
237	V432 Mon	NGC 2264	9.85	6.1	11	
238	MO Mon	NGC 2264	9.85	4.8	11	

TABLE III (Continued)

HRC	STAR	LOCATION	$(m-M)_{pg}$	M_{pg}	REFERENCE	NOTE
239	OW Mon	NGC 2264	9.85	6.0	11	
240	OY Mon	NGC 2264	9.85	5.0	11	
241	MQ Mon	NGC 2264	9.85	5.9	11	
242	PY Mon	NGC 2264	9.85	4.7	11	
97	San 1	Orion neb	9.1	3.9	12	14
98	HS Ori	Orion neb	9.1	6.6	12	
99	HT Ori	Orion neb	9.1	5.3	12	
100	V466 Ori	Orion neb	9.1	4.6	12	
102	P 1207	Orion neb	9.1	5.6	12	
103	VX Ori	Orion neb	9.1	6.7	12	
104	VY Ori	Orion neb	9.1	6.8	12	
105	San 2	Orion neb	9.1	4.9	12	
106	VZ Ori	Orion neb	9.1	5.5	12	
107	V386 Ori	Orion neb	9.1	7.5	12	
108	P 1267	Orion neb	9.1	5.4	12	
109	P 1270	Orion neb	9.1	3.8	12	
110	Su Ori	Orion neb	9.1	6.7	12	
111	WX Ori	Orion neb	9.1	6.1	12	
113	P 1404	Orion neb	9.1	3.1	12	
114	EZ Ori	Orion neb	9.1	3.3	12	
115	SW Ori	Orion neb	9.1	5.6	12	
116	IU Ori	Orion neb	9.1	1.1	12	
117	XX Ori	Orion neb	9.1	6.7	12	
118	IX Ori	Orion neb	9.1	5.5	12	
119	YY Ori	Orion neb	9.1	5.2	12	

TABLE III (Continued)

HRC	STAR	LOCATION	$(m-M)_{pg}$	M_{pg}	REFERENCE	NOTE
120	YZ Ori	Orion neb	9.1	6.4	12	
121	P 1649	Orion neb	9.1	2.1	12	
122	KM Ori	Orion neb	9.1	3.9	12	
123	KN Ori	Orion neb	9.1	5.3	12	
124	KP Ori	Orion neb	9.1	6.4	12	
125	KR Ori	Orion neb	9.1	5.4	12	
126	LL Ori	Orion neb	9.1	3.5	12	
127	SY Ori	Orion neb	9.1	6.1	12	
128	LN Ori	Orion neb	9.1	7.1	12	
129	V356 Ori	Orion neb	9.1	6.2	12	
130	AA Ori	Orion neb	9.1	5.7	12	
131	V486 Ori	Orion neb	9.1	5.8	12	
132	P 1817	Orion neb	9.1	2.8	12	
133	LX Ori	Orion neb	9.1	4.0	12	
134	V488 Ori	Orion neb	9.1	4.9	12	
135	AB Ori	Orion neb	9.1	6.0	12	
136	TT Ori	Orion neb	9.1	5.7	12	
137	AD Ori	Orion neb	9.1	4.8	12	
138	P 1931	Orion neb	9.1	5.6	12	
139	P 1946	Orion neb	9.1	6.3	12	
140	AG Ori	Orion neb	9.1	5.6	12	
141	AI Ori	Orion neb	9.1	5.8	12	
142	NS Ori	Orion neb	9.1	7.3	12	
143	AL Ori	Orion neb	9.1	7.0	12	
144	V360 Ori	Orion neb	9.1	4.6	12	

TABLE III (Continued)

HRC	STAR	LOCATION	$(m-M)_{pg}$	M_{pg}	REFERENCE	NOTE
145	TW Ori	Orion neb	9.1	6.6	12	
146	AM Ori	Orion neb	9.1	5.7	12	
147	TV Ori	Orion neb	9.1	5.8	12	
148	NY Ori	Orion neb	9.1	6.9	12	
149	BO Ori	Orion neb	9.1	6.2	12	
150	AN Ori	Orion neb	9.1	3.6	12	
151	V573 Ori	Orion neb	9.1	6.8	12	
152	CE Ori	Orion neb	9.1	7.2	12	
153	OT Ori	Orion neb	9.1	6.1	12	
154	T Ori	Orion neb	9.1	1.2	12	
155	AR Ori	Orion neb	9.1	5.9	12	
156	V390 Ori	Orion neb	9.1	7.3	12	
157	AU Ori	Orion neb	9.1	6.5	12	
158	V577 Ori	Orion neb	9.1	6.4	12	
159	AV Ori	Orion neb	9.1	6.4	12	
160	PQ Ori	Orion neb	9.1	4.0	12	
161	PU Ori	Orion neb	9.1	4.4	12	
162	AZ Ori	Orion neb	9.1	5.9	12	
163	Haro 4-125	Orion neb	9.1	6.9	12	
165	BD Ori	Orion neb	9.1	5.4	12	
166	BC Ori	Orion neb	9.1	6.5	12	
167	P 2441	Orion neb	9.1	2.2	12	
168	BE Ori	Orion neb	9.1	6.1	12	
169	BF Ori	Orion neb	9.1	1.8	12	
172	TX Ori	Orion neb	9.1	5.6	12	

TABLE III (Continued)

HRC	STAR	LOCATION	$(m-M)_{pg}$	M_{pg}	REFERENCE	NOTE
173	TY Ori	Orion neb	9.1	6.2	12	
174	Haro 7-1	Orion neb	9.1	4.9	12	
175	Haro 7-5	Orion neb	9.1	5.9	12	
176	Haro 4-255	Orion neb	9.1	5.9	12	
177	V510 Ori	Orion neb	9.1	5.6	12	
178	BH Ori	Orion neb	9.1	5.4	12	
179	Haro 7-4	Orion neb	9.1	5.9	12	
181	DL Ori	Orion neb	9.1	4.4	12	
182	Haro 7-2	Orion neb	9.1	3.9	12	
188	Lk Hα 334	Orion neb	9.1	5.9	12	
189	Lk Hα 335	Orion neb	9.1	6.9	12	
190	Lk Hα 336	Orion neb	9.1	6.9	12	
191	Lk Hα 337	Orion neb	9.1	4.9	12	

References:

1. Johnson, 1968
2. Johnson, et al., 1961
3. Herbig, 1960
4. Buscombe, 1963
5. Herbig, 1971
6. Kholopov, 1959
7. Imhoff and Mendoza, 1974
8. Allen, 1973
9. Kuhi, 1964
10. Rydgren, Strom, and Strom, 1975
11. Walker, 1956
12. Penston and Hunter, 1975

TABLE III (Continued)

Notes:

1. ADN for anonymous dark nebula.
2. Adopted from the distance modulus for FU Ori (HRC 186).
3. Assumed $A_B = 0.1$.
4. Actually $4.0 = M_V$ not M_B.
5. Distance modulus adopted from the average modulus calculated from ρ Oph stars discussed in Rydgren, Strom, and Strom, 1975.
6. Adopted the distance modulus for V1057 Cyg (HRC 300).
7. Adopted the distance modulus for Cep IV as that of Cep III.
8. Adopted from average distance modulus calculated for B209.
9. Adopted from average distance modulus calculated for B7.
10. Adopted from average distance modulus calculated for B19.
11. By proximity to DI Tau (HRC 39), adopted the same distance modulus.
12. Adopted from average distance modulus calculated for B18.
13. After examination of Palomar Sky Survey Prints and considering the absorptions of the stars in Rydgren, Strom, and Strom, 1975, the star was assigned to one of three groups on the basis of an estimation of the visible absorption in the immediate area. An average distance modulus for either light, moderate or heavy absorption was adopted.
14. Adopted the distance modulus based on the average of the absorptions in Penston and Hunter, 1975.

LICRV		EMINT 0.0	1.00	2.00	3.00	4.00	5.00	ROW TOTAL
	COUNT	NO EMISS ION	ONLY H LINE ALPHA	WEAKLINE H & CAII IN PHO	H & CAII MODERAT	ADVANCED STRONG	T-TAURI	
1. MF BRT	THN FNT	2	14	13	1	0	0	30
	ROW PCT	6.7	46.7	43.3	3.3	0.0	0.0	24.8
	COL PCT	22.2	50.0	37.1	3.8	0.0	0.0	
	TOT PCT	1.7	11.6	10.7	0.8	0.0	0.0	
2. MF HAS	MEAN BRT	3	7	3	9	9	4	35
	ROW PCT	8.6	20.0	8.6	25.7	25.7	11.4	28.9
	COL PCT	33.3	25.0	8.6	34.6	60.0	50.0	
	TOT PCT	2.5	5.8	2.5	7.4	7.4	3.3	
3. MF FNT	THN BRT	2	4	11	9	4	1	31
	ROW PCT	6.5	12.9	35.5	29.0	12.9	3.2	25.6
	COL PCT	22.2	14.3	31.4	34.6	26.7	12.5	
	TOT PCT	1.7	3.3	9.1	7.4	3.3	0.8	
4. NO PREF	ANY LEV	2	3	8	7	2	3	25
	ROW PCT	8.0	12.0	32.0	28.0	8.0	12.0	20.7
	COL PCT	22.2	10.7	22.9	26.9	13.3	37.5	
	TOT PCT	1.7	2.5	6.6	5.8	1.7	2.5	
	COLUMN TOTAL	9	28	35	26	15	8	121
		7.4	23.1	28.9	21.5	12.4	6.6	100.0

TABLE IV. TWO-WAY FREQUENCY DISTRIBUTION OF THE LIGHT CURVE CLASSIFICATION AND EMISSION INTENSITY. CASES WITH INTERMEDIATE VALUES OF THE EMISSION INTENSITY HAVE BEEN INCLUDED WITH THE NEXT GREATEST VALUE.

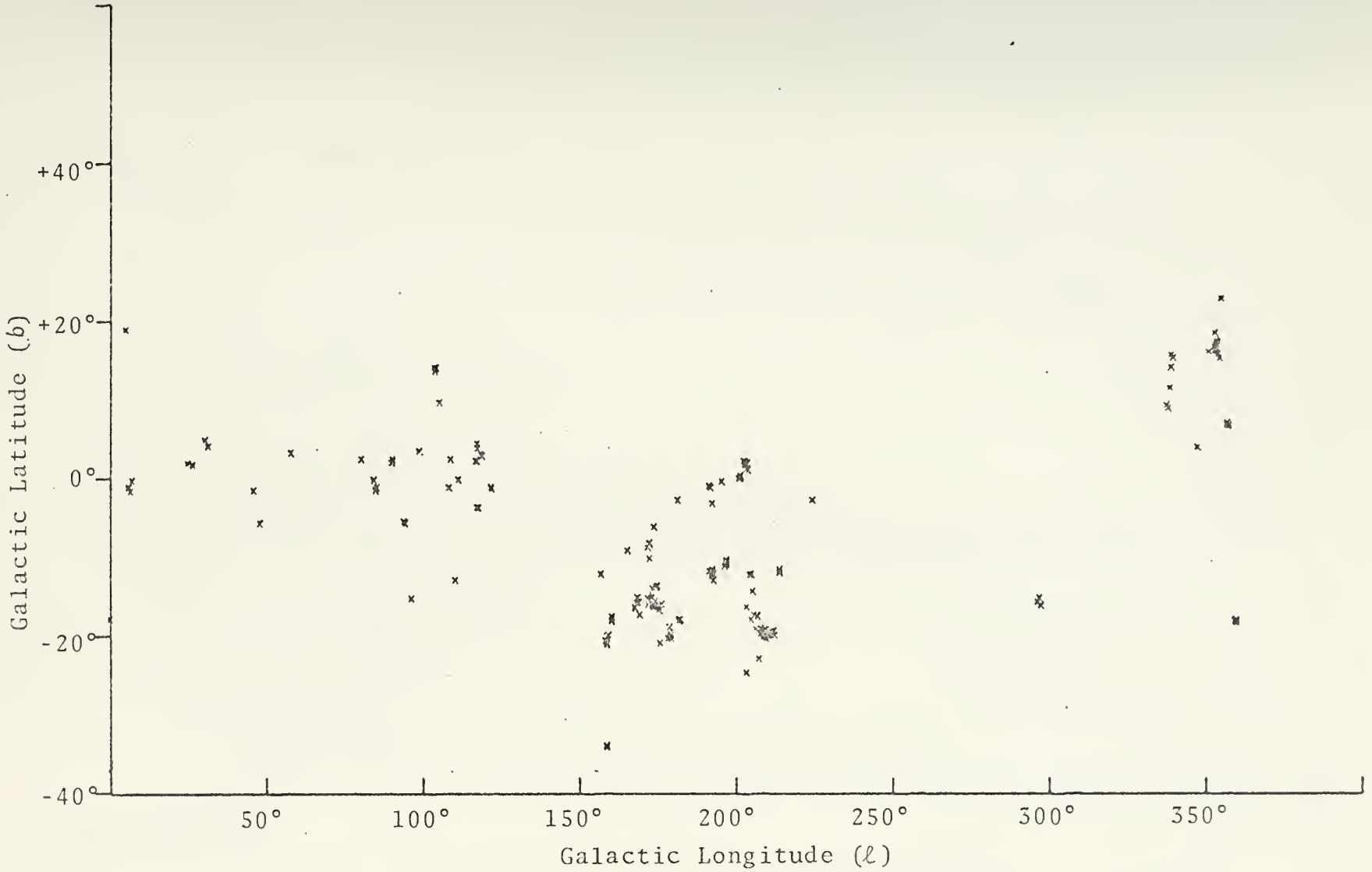

Figure 1. Two dimensional plot showing the position of all Catalog stars in a galactic coordinate system.

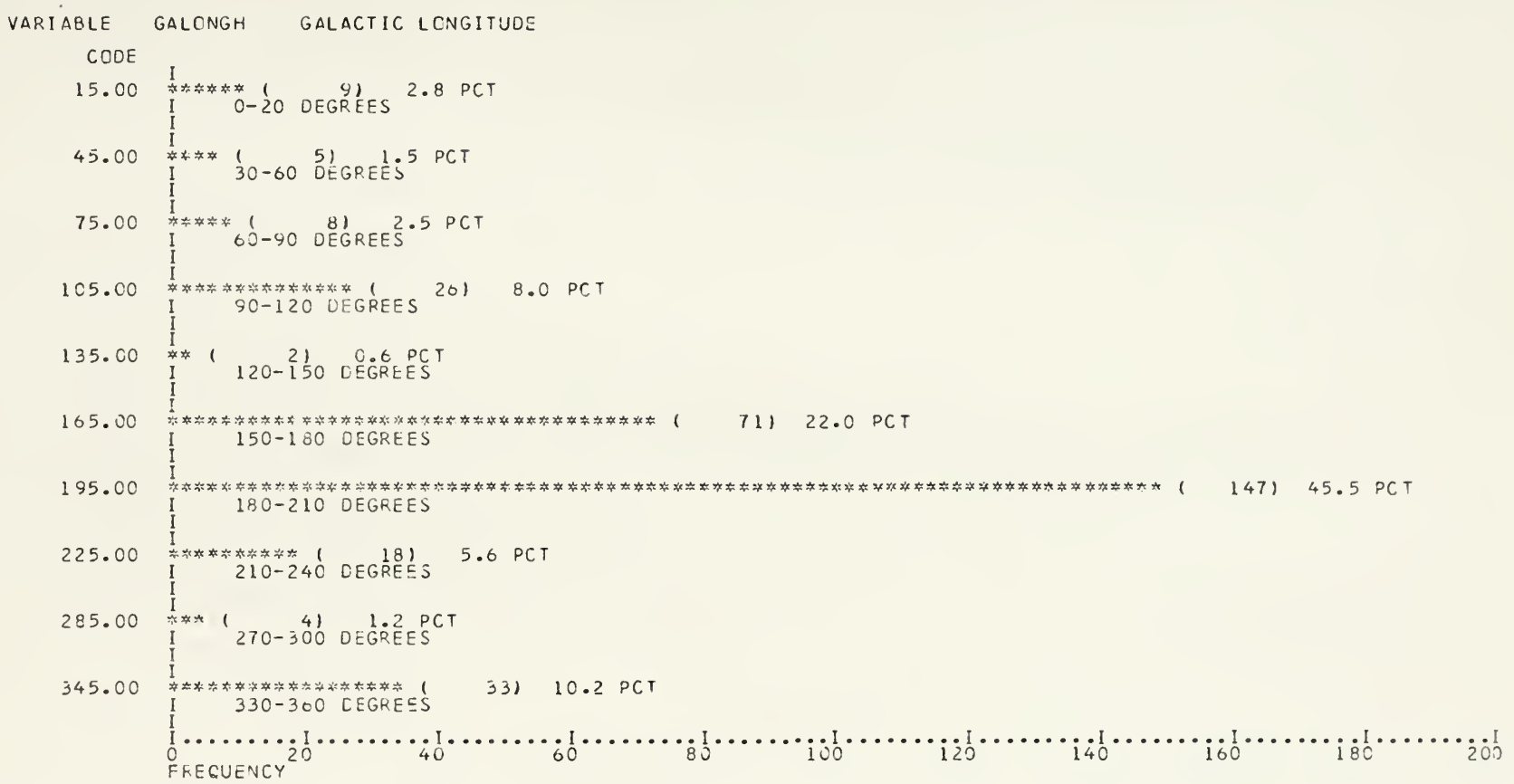

Figure 2- Histogram of Galactic Longitude.

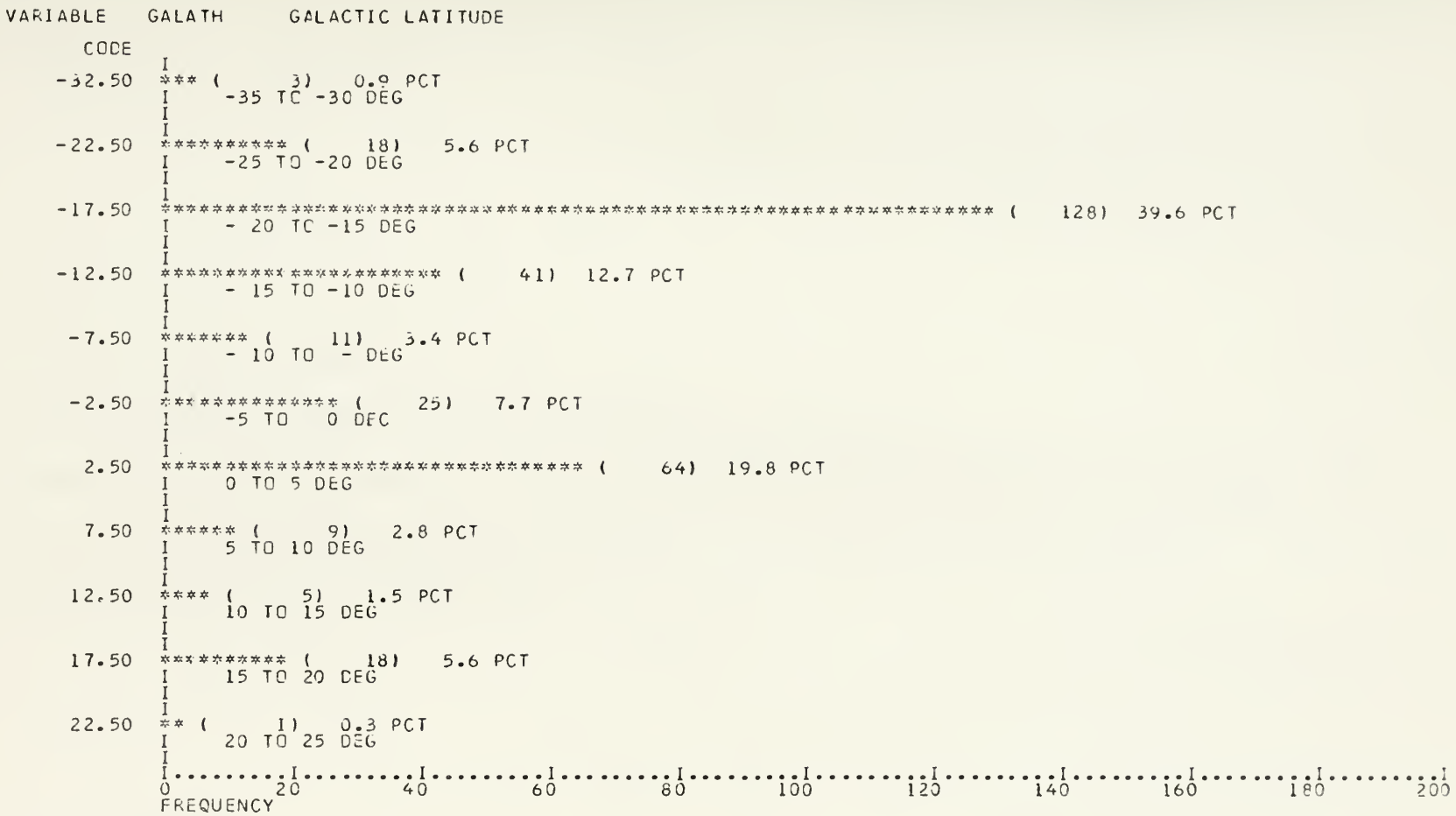

Figure 3- Histogram of Galactic Latitude.

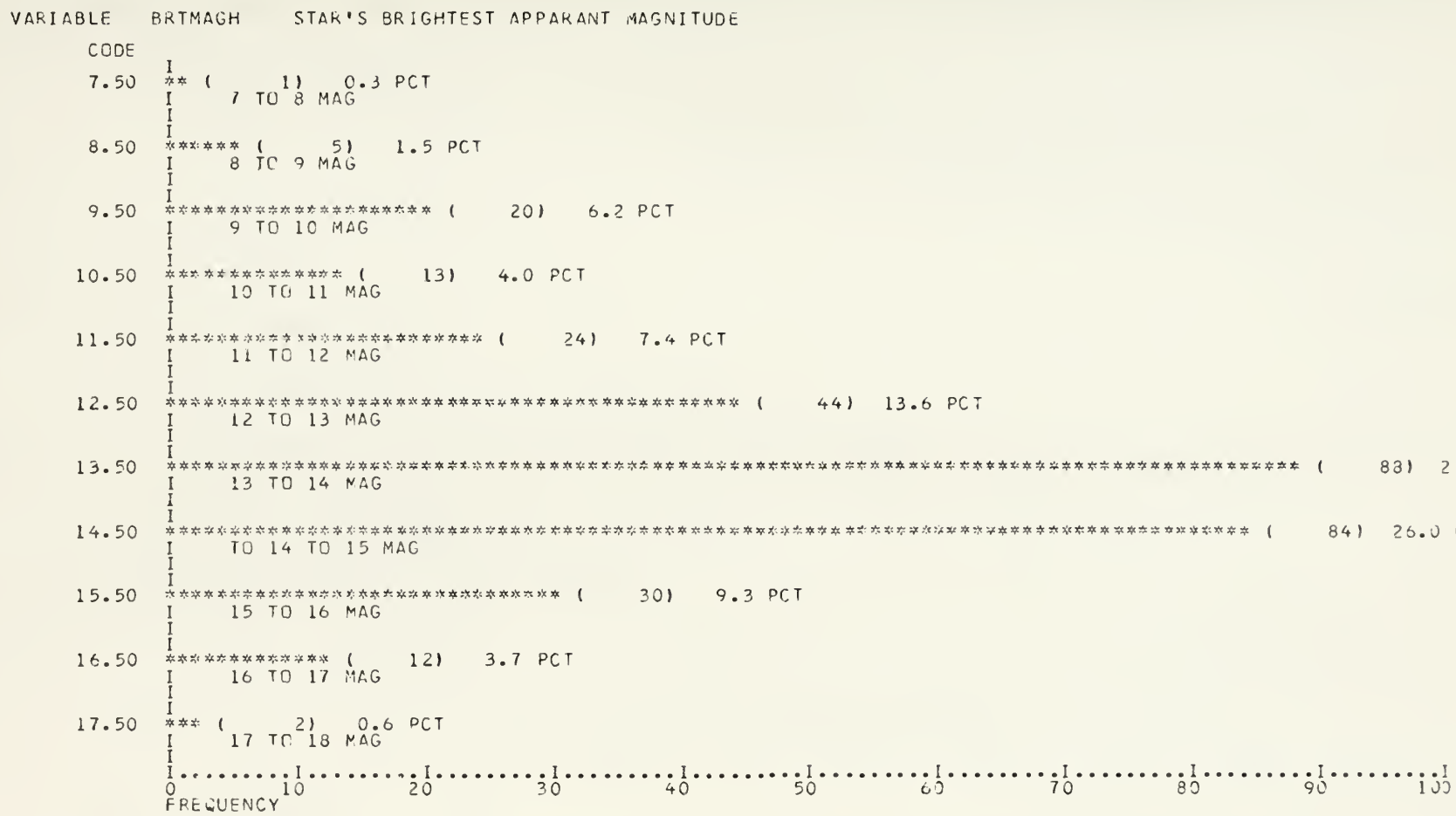

Figure 4- Histogram of Brightest Apparent Magnitude.

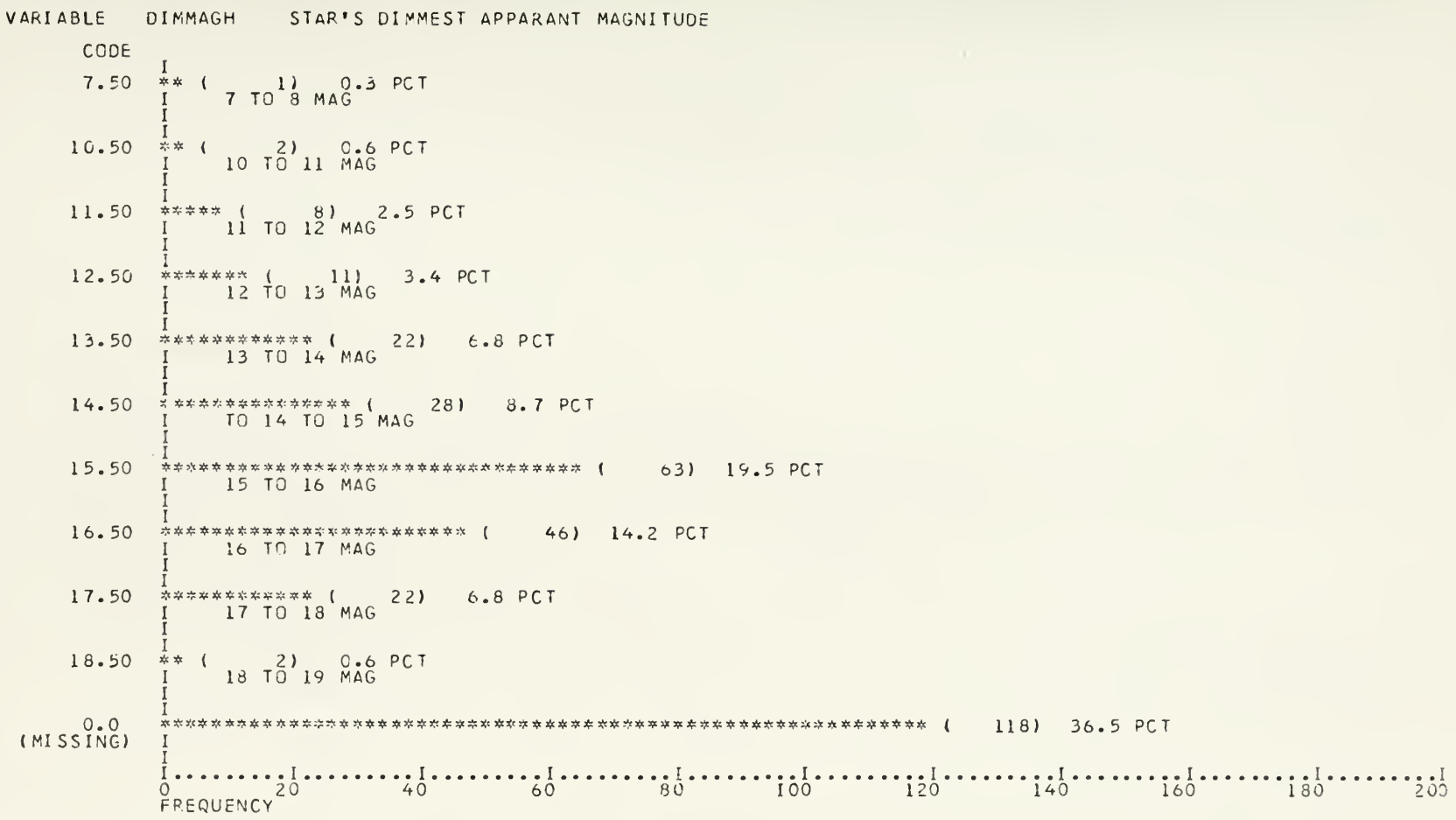

Figure 5- Histogram of Dimmest Apparent Magnitude.

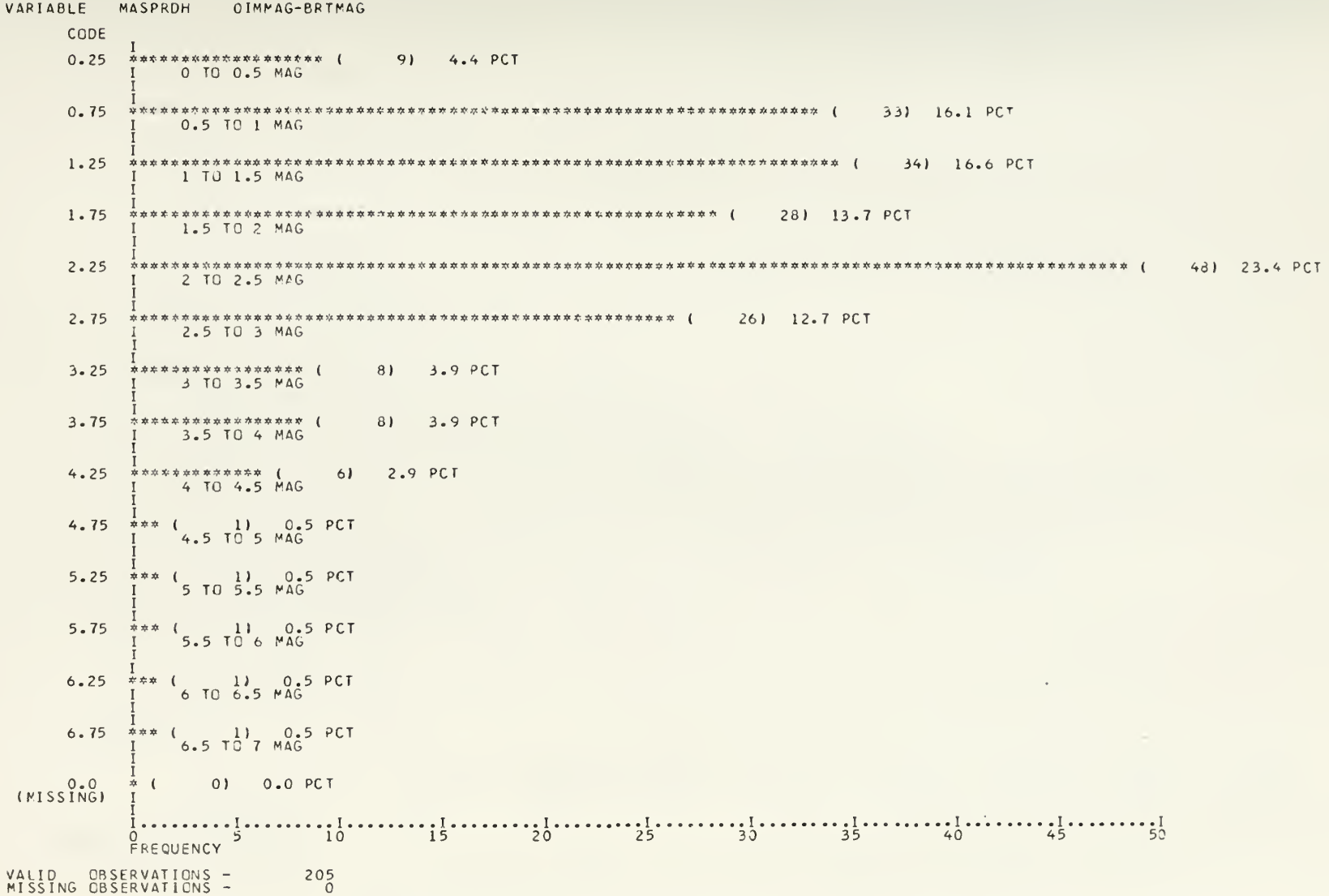

Figure 6- Histogram of the Range of Apparent Magnitude for Those Catalog Stars with such a Range Defined.

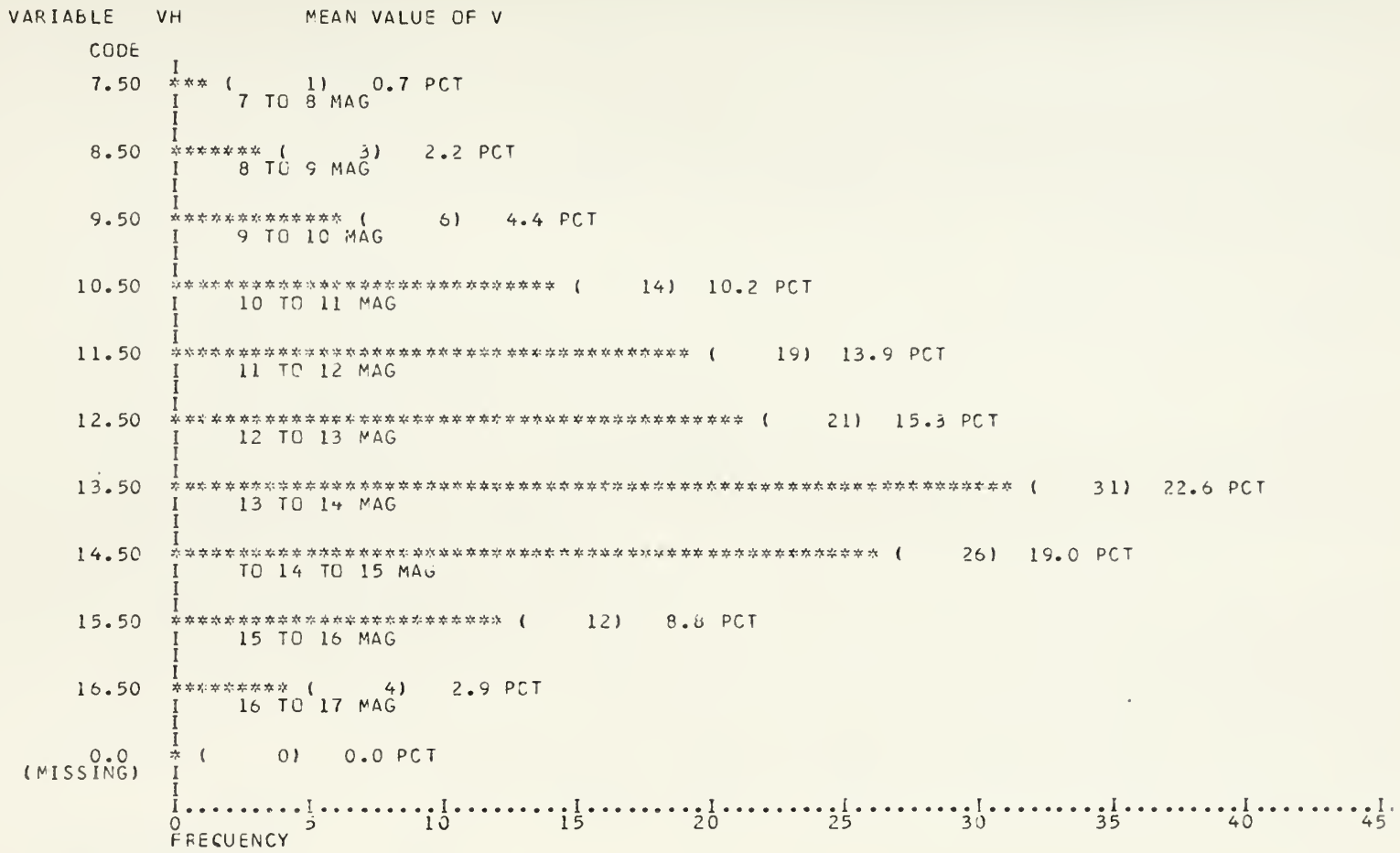

Figure 7- Histogram of V for Those Catalog Stars with V Photometry.

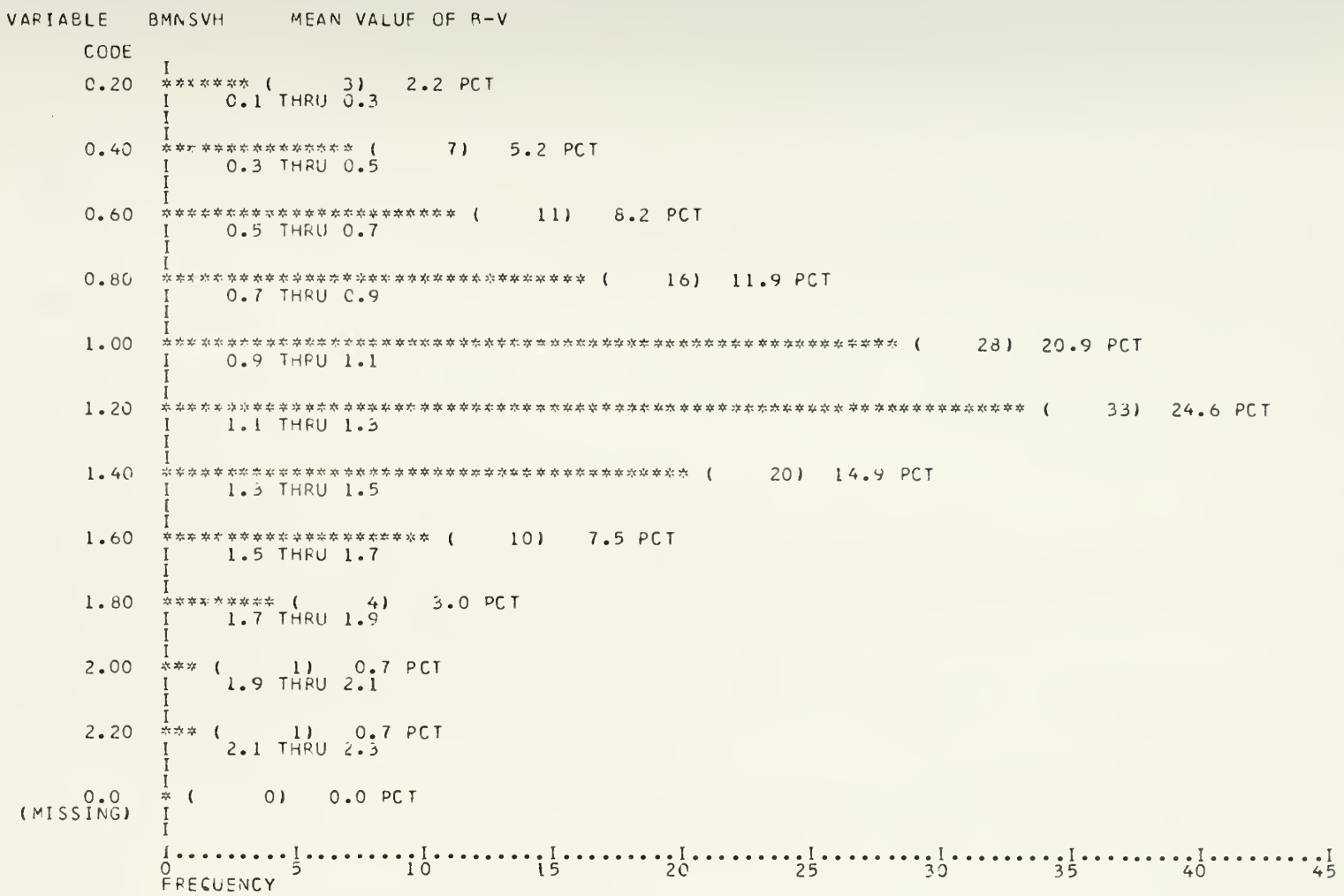

Figure 8- Histogram of B-V for those stars with B-V photometry.

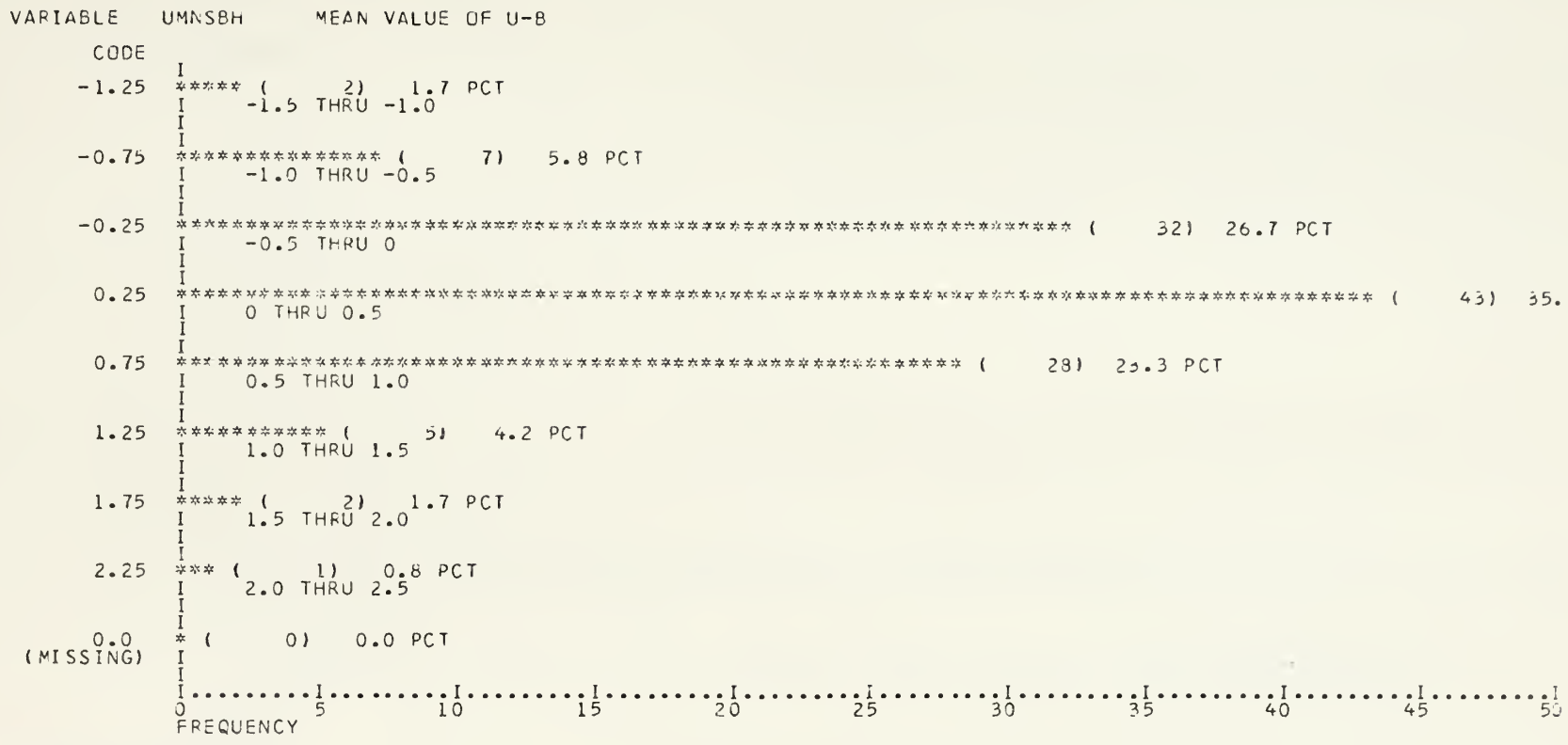

Figure 9- Histogram of U-B for those Catalog stars with U-B photometry.

```
VARIABLE   SPCLAS     ROUGH SPECTRAL CLASS

      CODE
                I
      2.00      ******** (      7)   2.3 PCT
                I     B TYPE
                I
                I
      3.00      ********** (      9)   2.9 PCT
                I     A TYPE
                I
                I
      4.00      ************** (     14)   4.6 PCT
                I     F TYPE
                I
                I
      5.00      ********************************************** (     42)  13.7 PCT
                I     G TYPE
                I
                I
      6.00      ************************************************************************** (     75)  24.5 PCT
                I     K TYPE
                I
                I
      7.00      ************************** (     28)   9.2 PCT
                I     M TYPE
                I
                I
     99.00      ******** (      7)   2.3 PCT
                I     CLASS   G-K
                I
                I
     99.10      *** (      2)   0.7 PCT
                I     CLASS   K-M
                I
                I
     99.20      *** (      2)   0.7 PCT
                I     CLASS   A-F
                I
                I
     99.30      **** (      3)   1.0 PCT
                I     CLASS   B-A
                I
                I
     99.80      ************************************************************************************** (     97)  31.7 PCT
                I     APPEARS CONT.
                I
                I
     99.90      ******************** (     20)   6.5 PCT
                I     CLEARLY CONT.
                I
                I.........I.........I.........I.........I.........I.........I.........I.........I.........I
                0         10        20        30        40        50        60        70        80        90        100
                FREQUENCY

VALID   OBSERVATIONS -      306
MISSING OBSERVATIONS -        0
```

Figure 10- Histogram of Spectral Class for all Catalog stars with a cataloged spectrum.

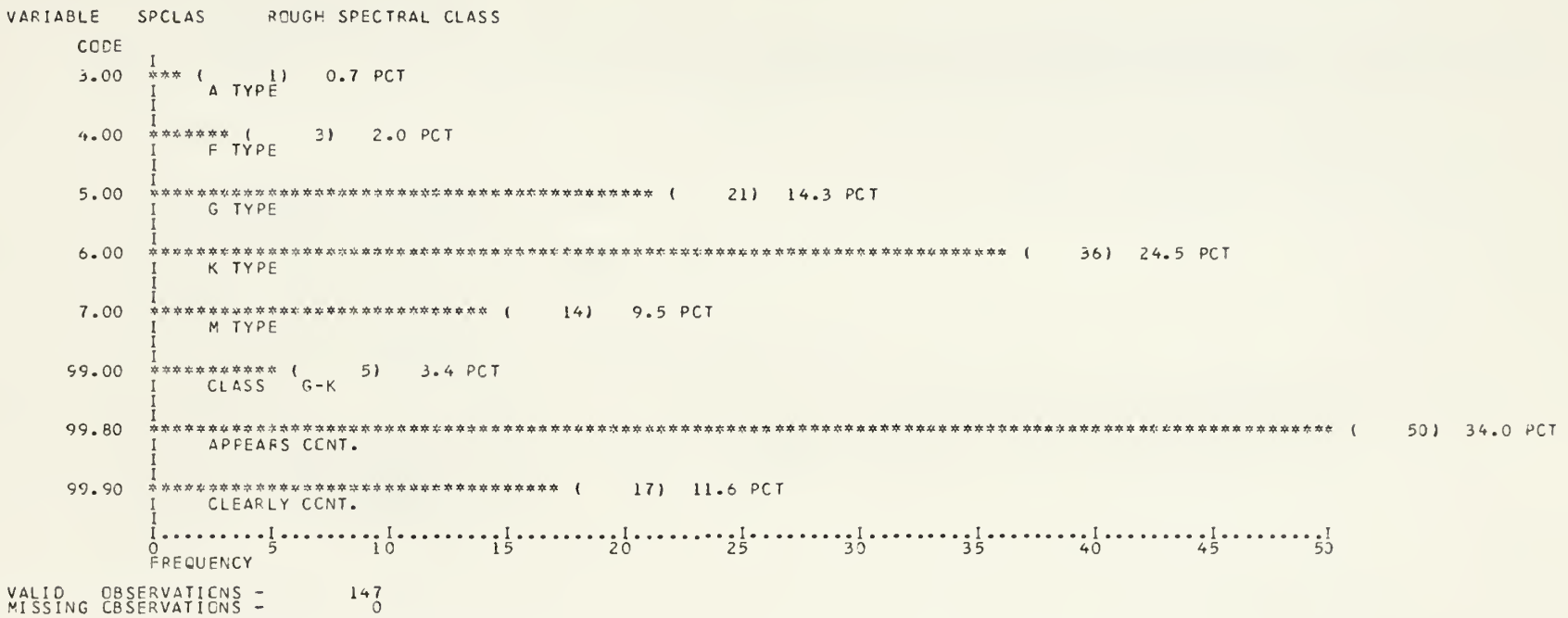

Figure 11- Histogram of Spectral Class for certain or possible T Tauri stars.

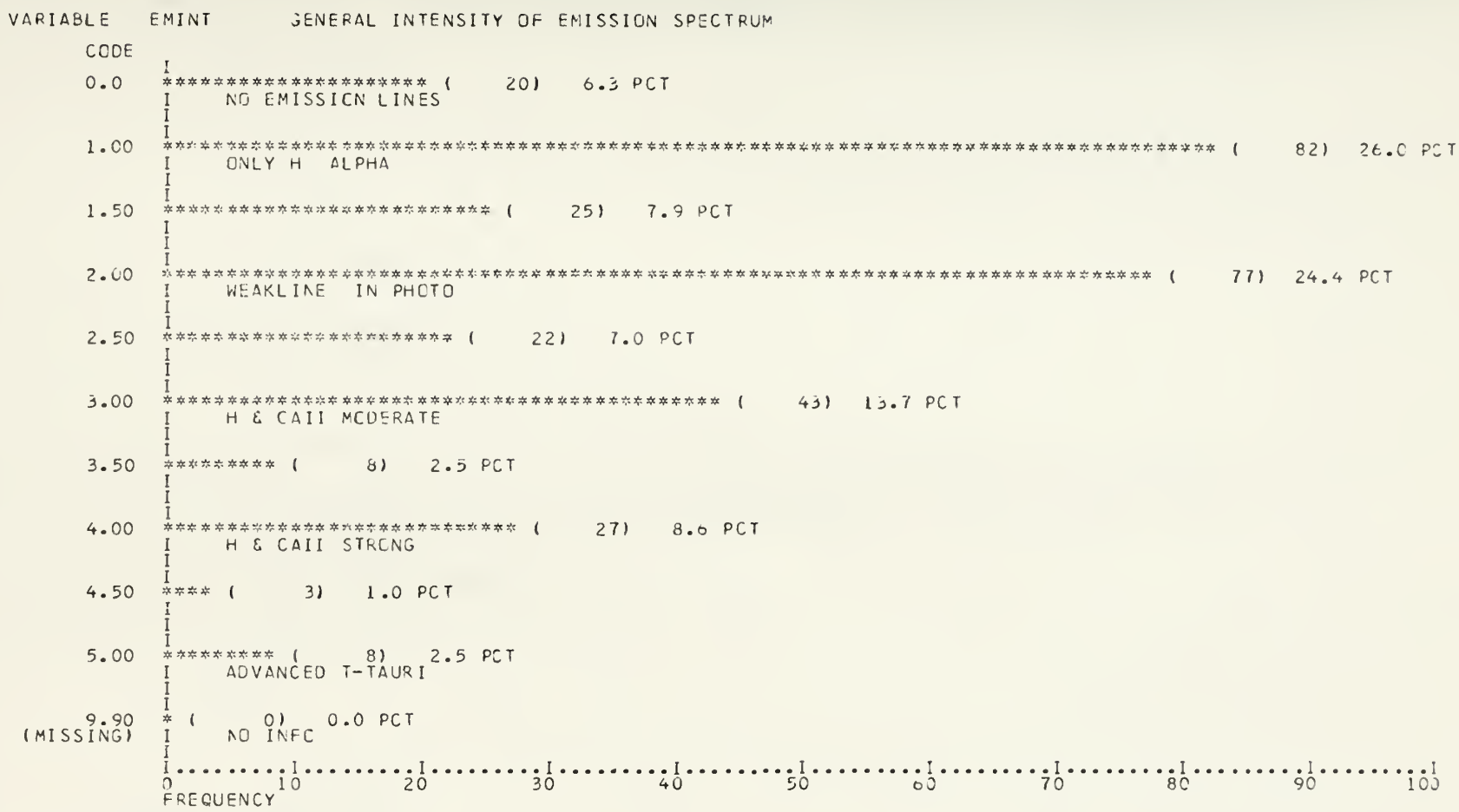

Figure 12- Histogram of emission intensities for all Catalog stars with a listed value.

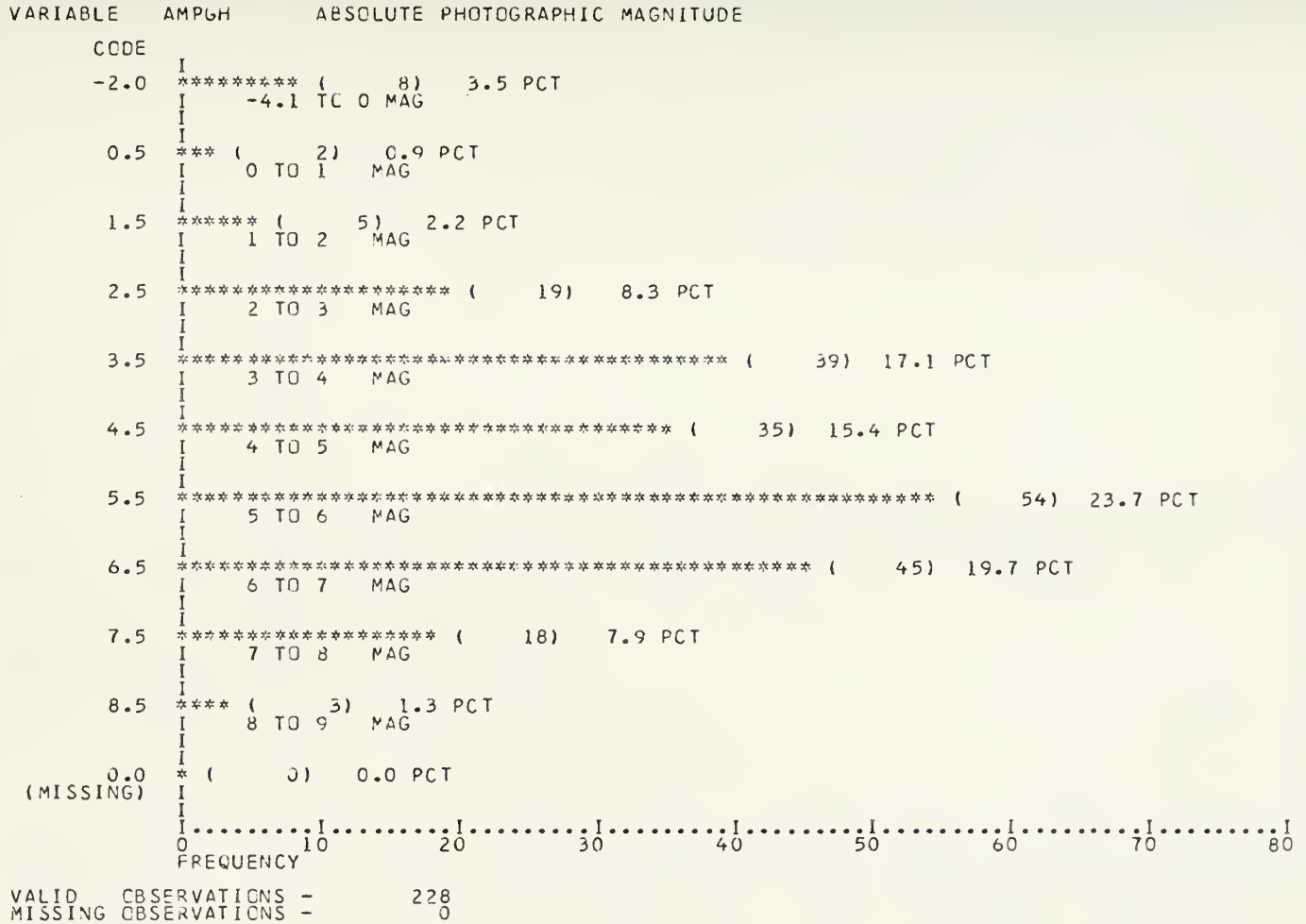

Figure 13- Histogram of absolute photographic magnitude for those Catalog stars for which a value could be determined.

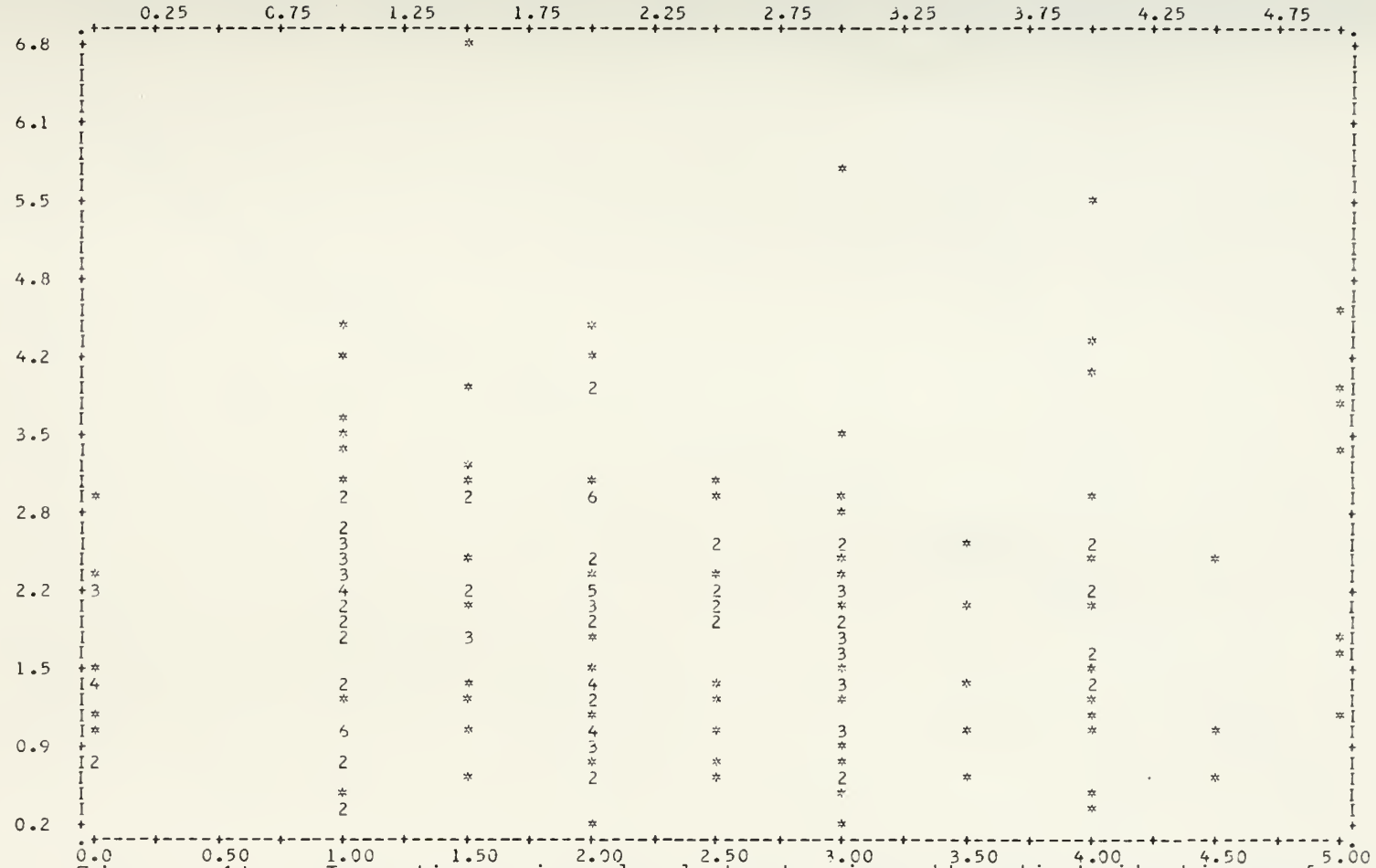

Figure 14- Two dimensional plot showing the distribution of the range in absolute magnitude for each value of emission intensity. Each asterisk indicates a single star, numbers indicate the number of multiple values. Those stars without one of the values are not plotted. Stars plotted- 203.

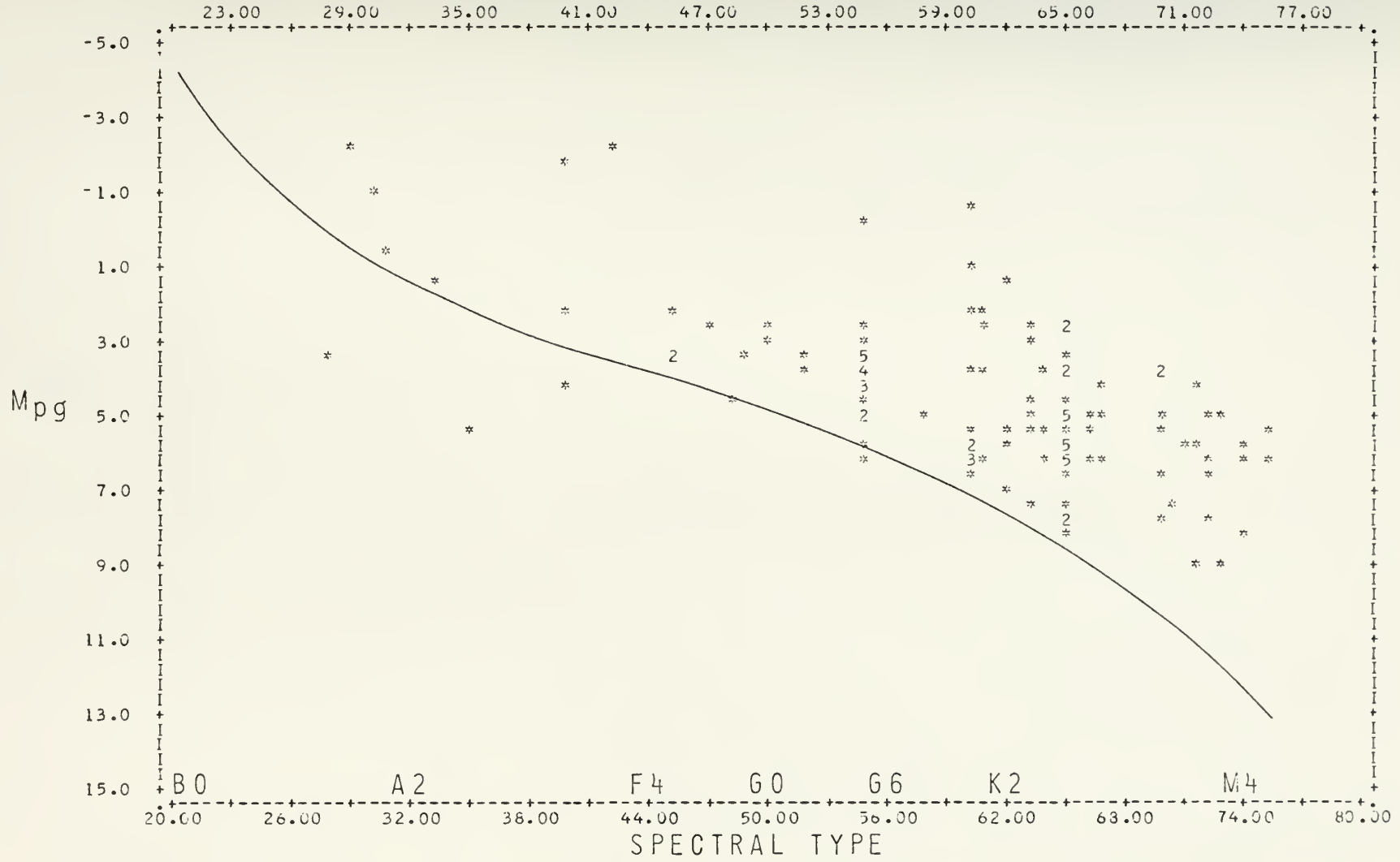

Figure 15- H-R diagram for all Catalog stars with a tabulated spectrum and determined absolute photographic magnitude (Mpg). Plotted values- 124. The solid line is the dwarf main sequence.

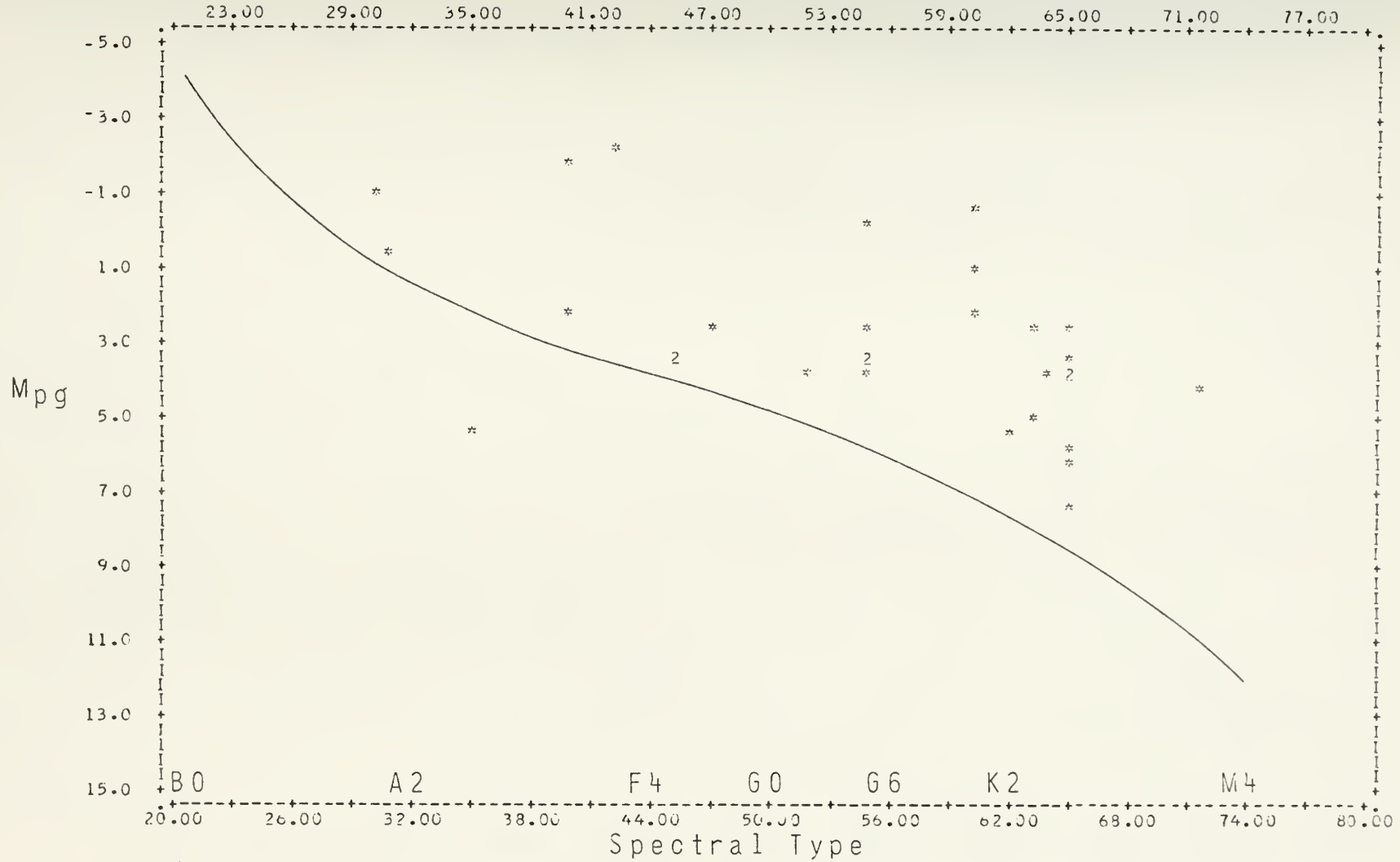

Figure 16- H-R diagram for the Catalog stars not members of the asterisms Taurus-Auriga, NGC-2264 and Orion. Plotted values- 30.

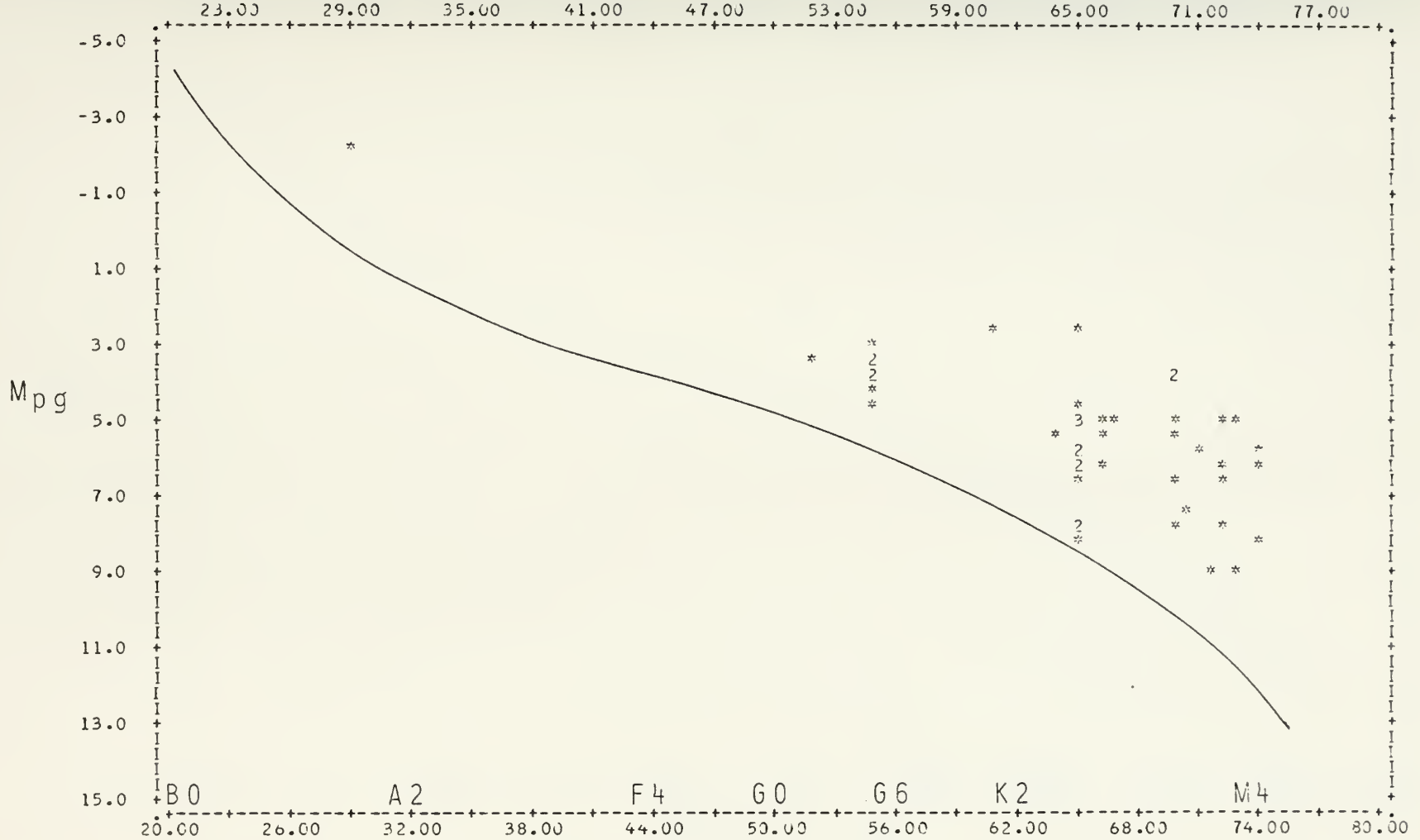

Figure 17- H-R diagram for the Catalog stars in the asterism Taurus-Auriga. Plotted values- 46.

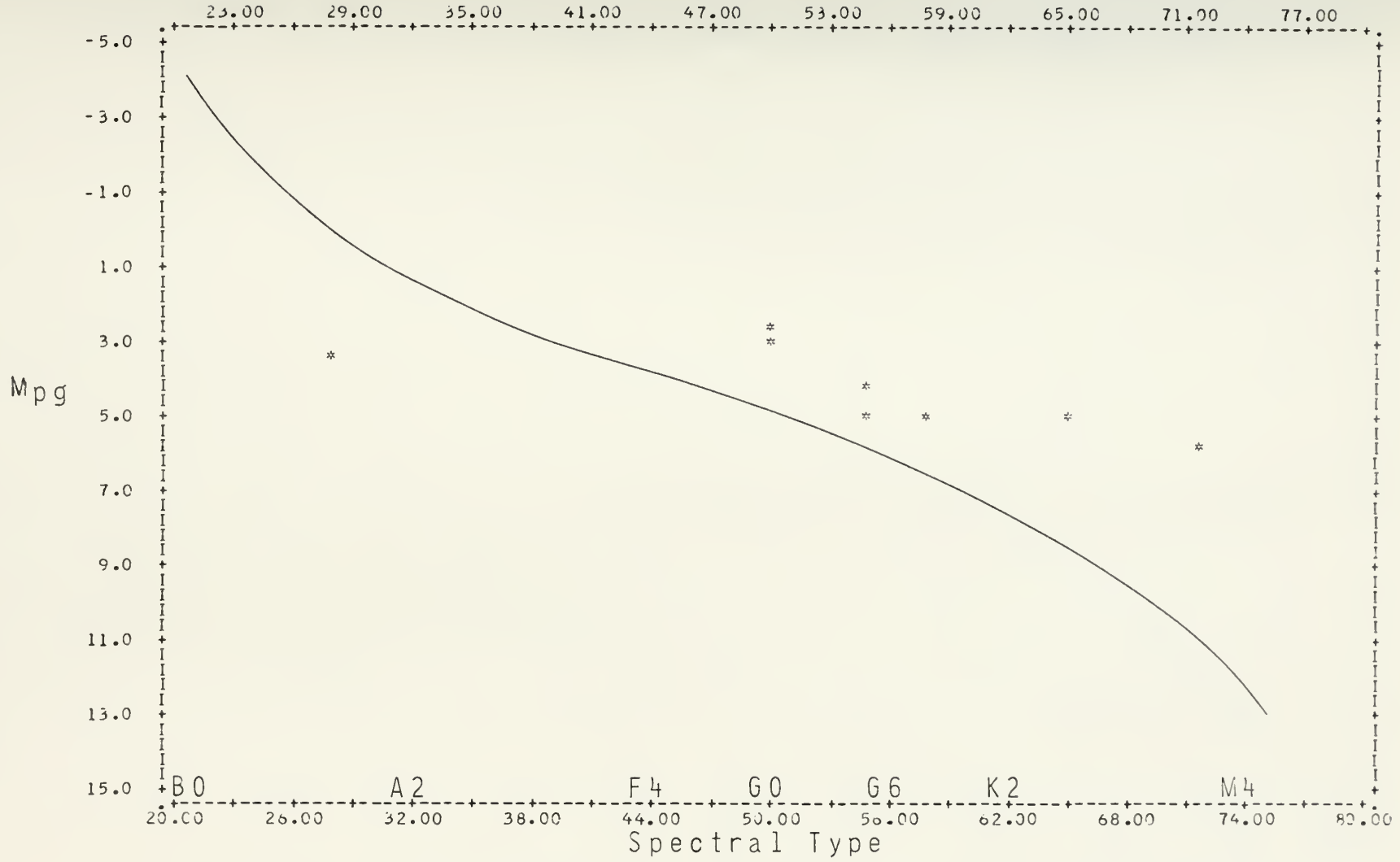

Figure 18- H-R diagram for the Catalog stars in the cluster NGC 2264. Plotted values- 8.

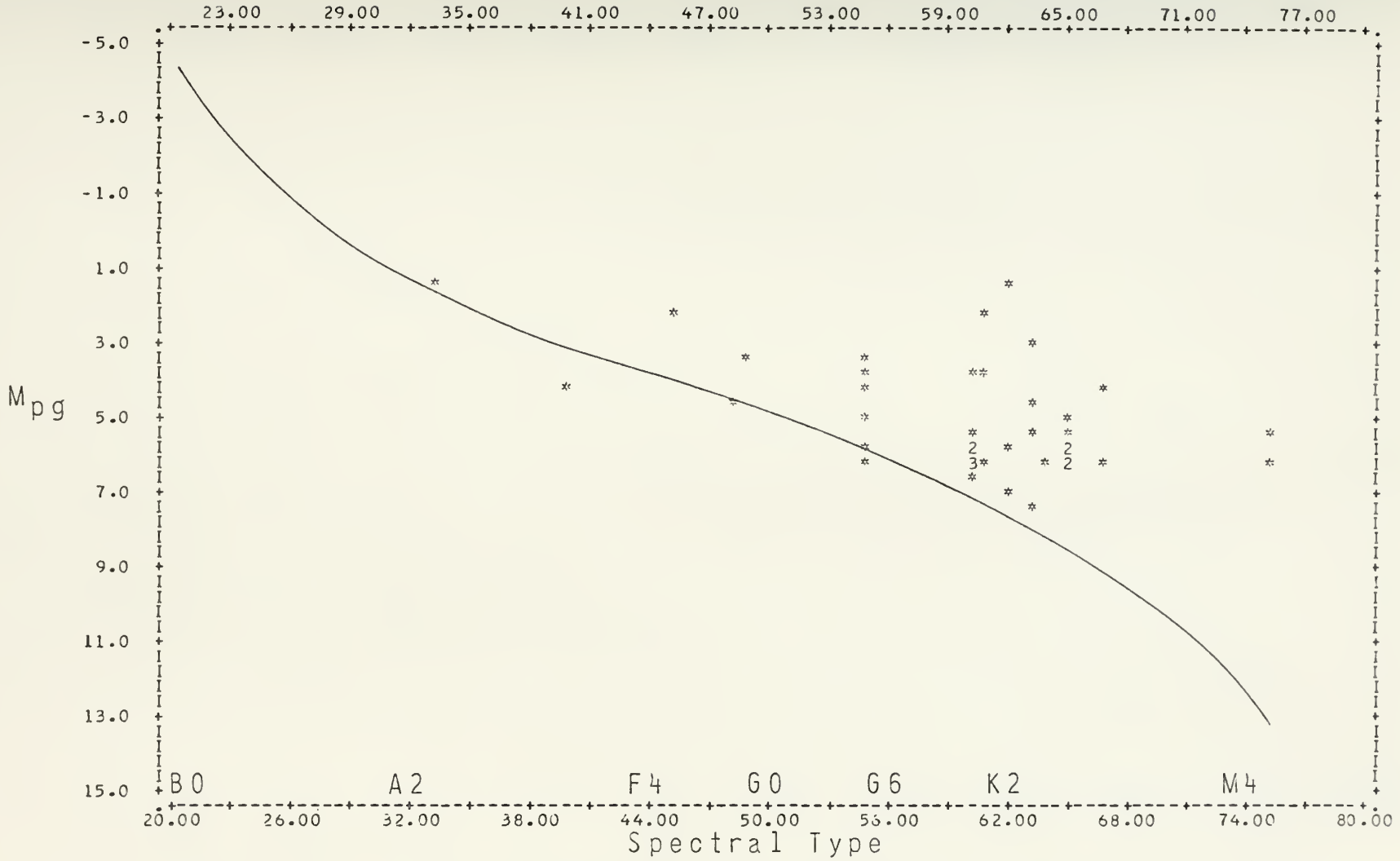

Figure 19- H-R diagram for the Catalog stars in the Orion asterism. Plotted values- 40.

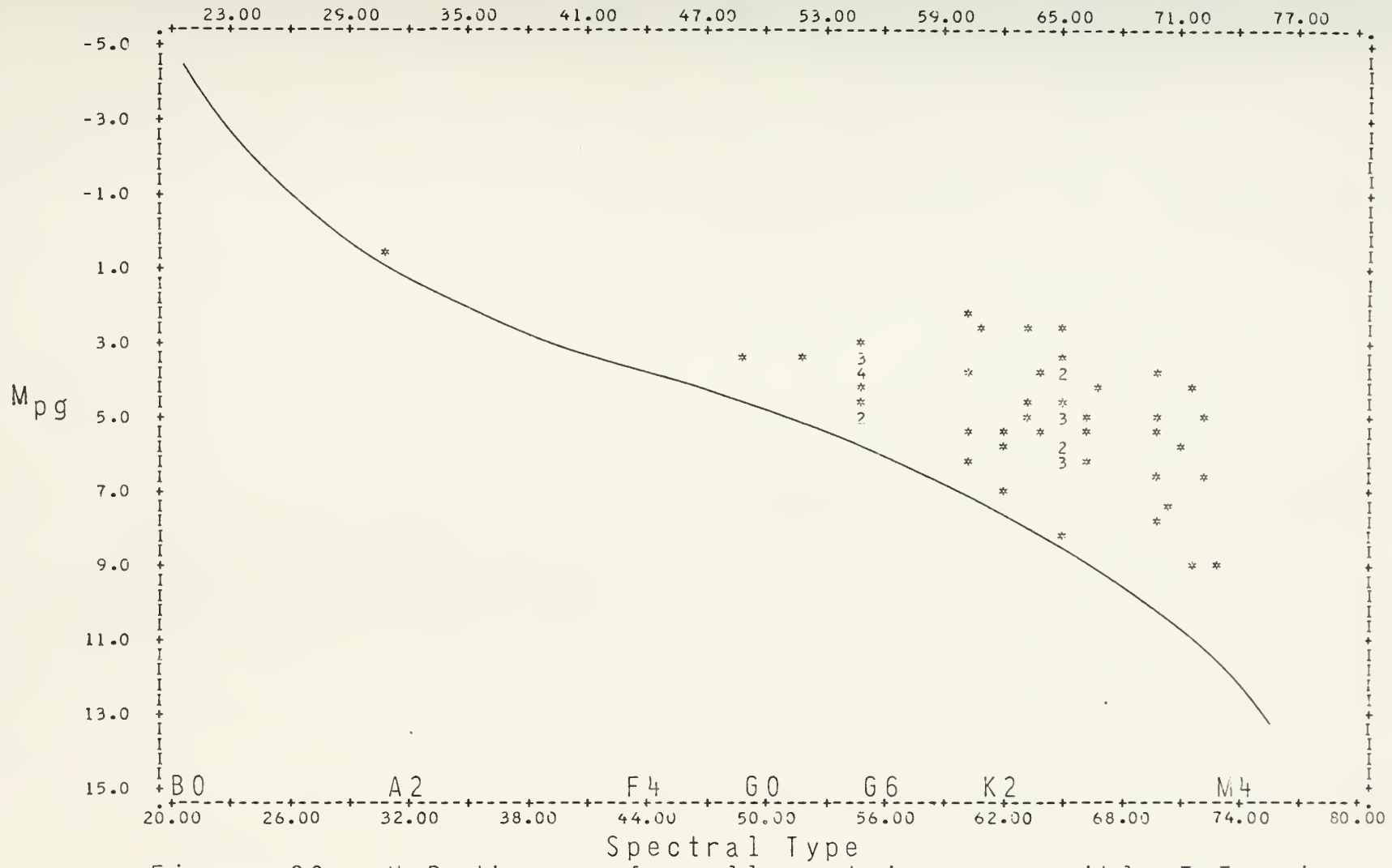

Figure 20- H-R diagram for all certain or possible T Tauri stars in the Catalog. Plotted values- 58.

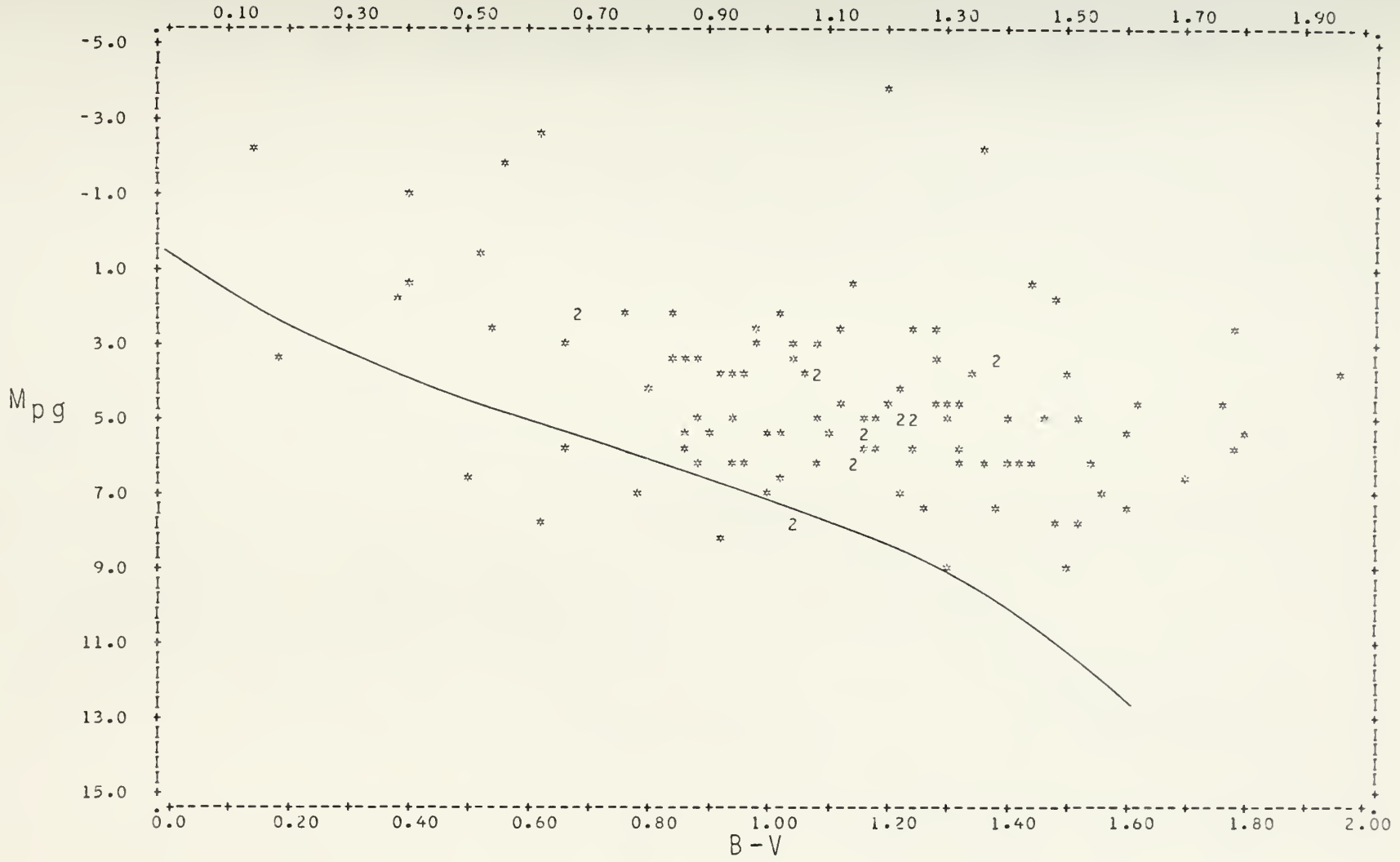

Figure 21- H-R diagram for all Catalog stars with both B-V photometry and a determined absolute photographic magnitude (M_{pg}). Plotted values- 112. The solid line is the dwarf main sequence.

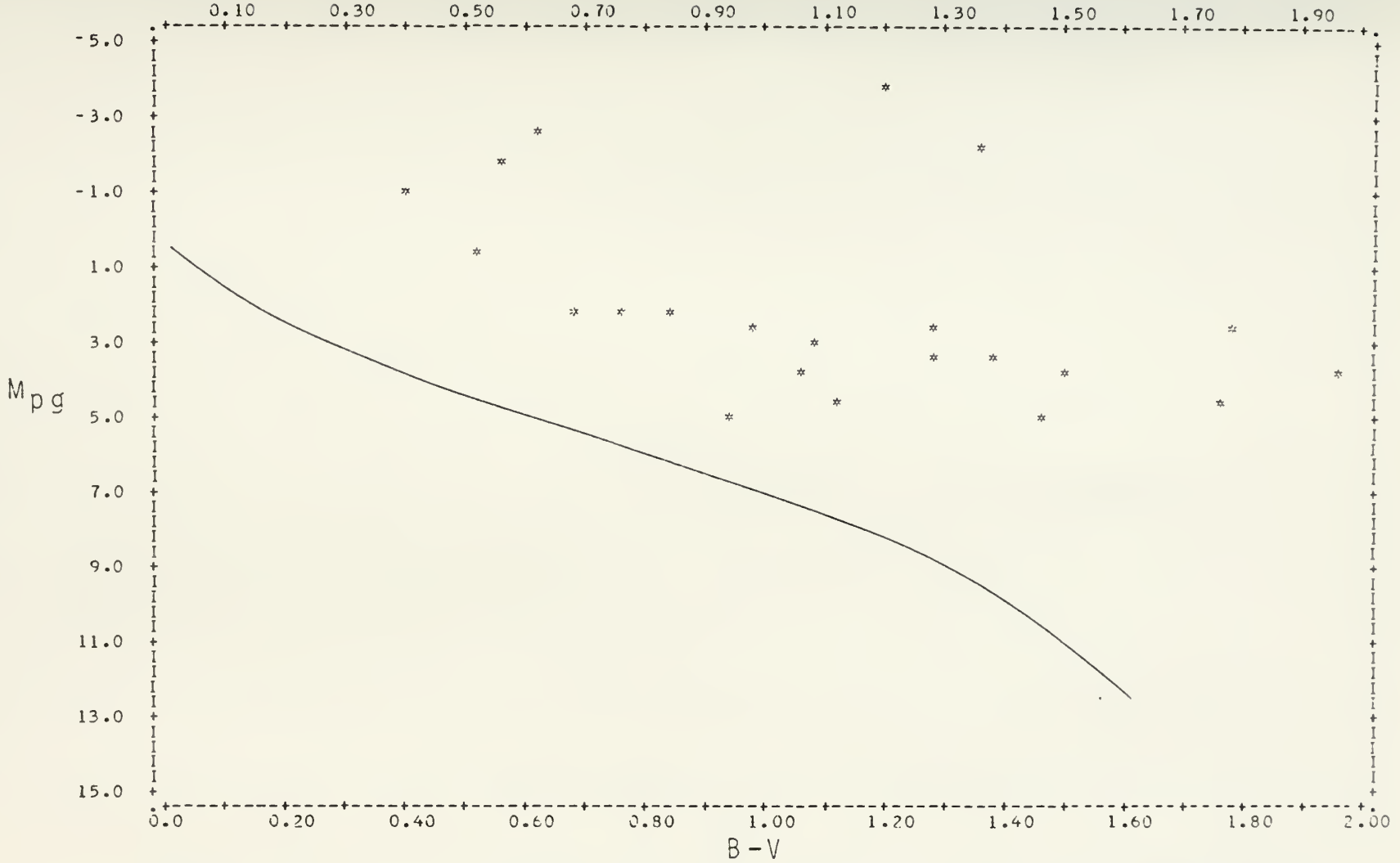

Figure 22- H-R diagram for the Catalog stars not members of the asterisms Taurus-Auriga, NGC-2264 or Orion. Plotted values- 22.

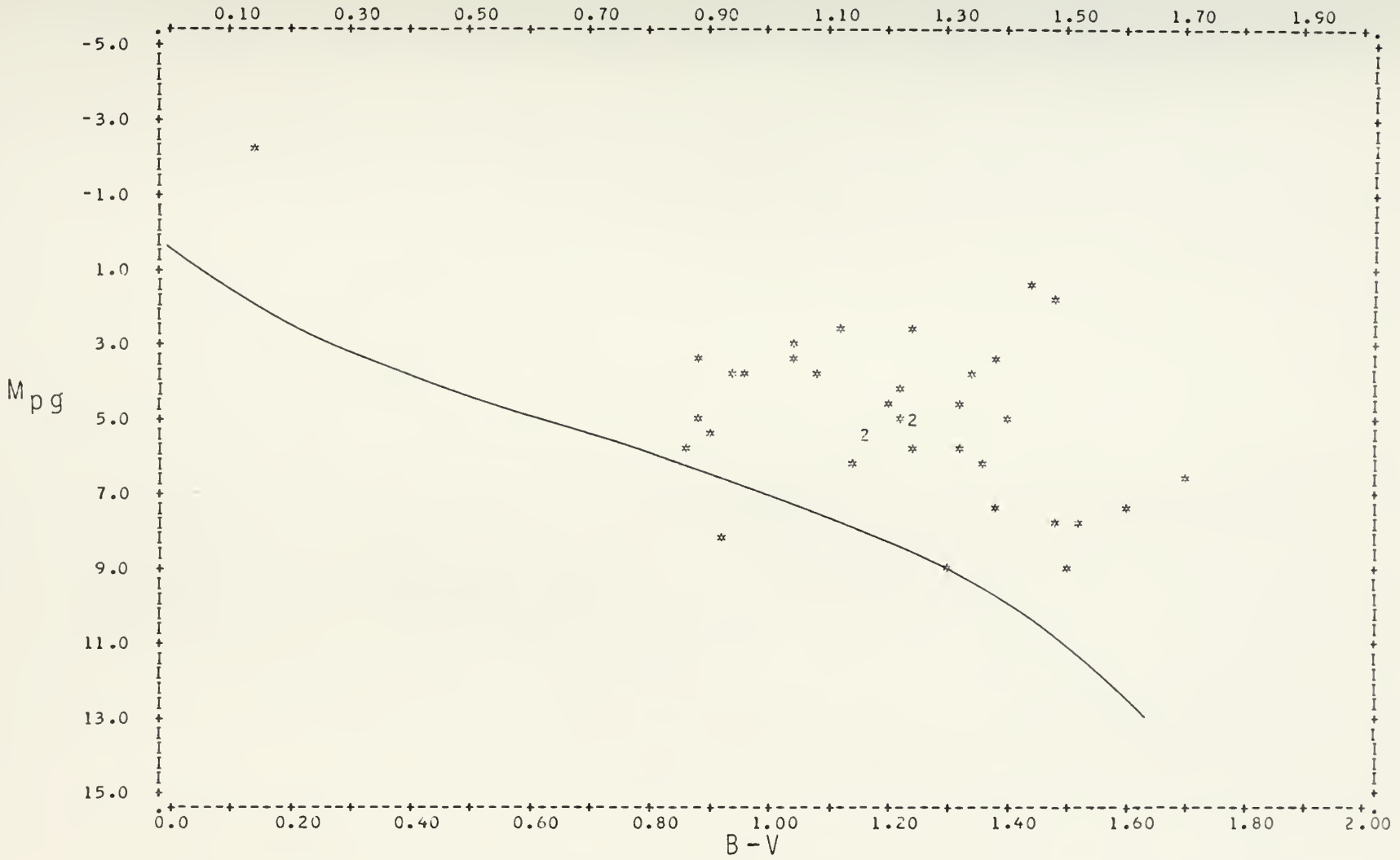

Figure 23- H-R diagram for the Catalog stars in the Taurus-Auriga asterism. Plotted values- 37.

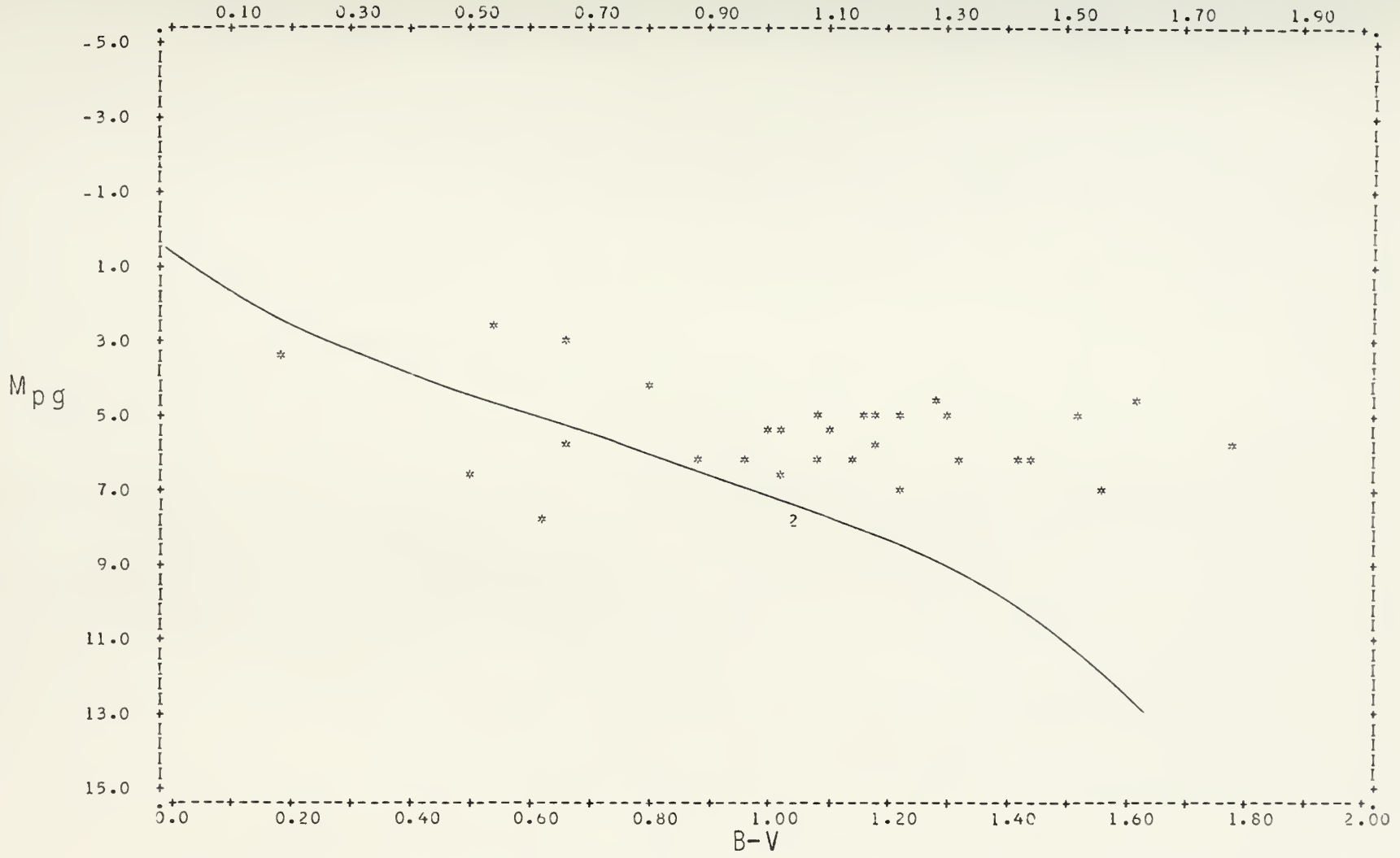

Figure 24- H-R diagram for the Catalog stars in the cluster NGC-2264. Plotted values- 32.

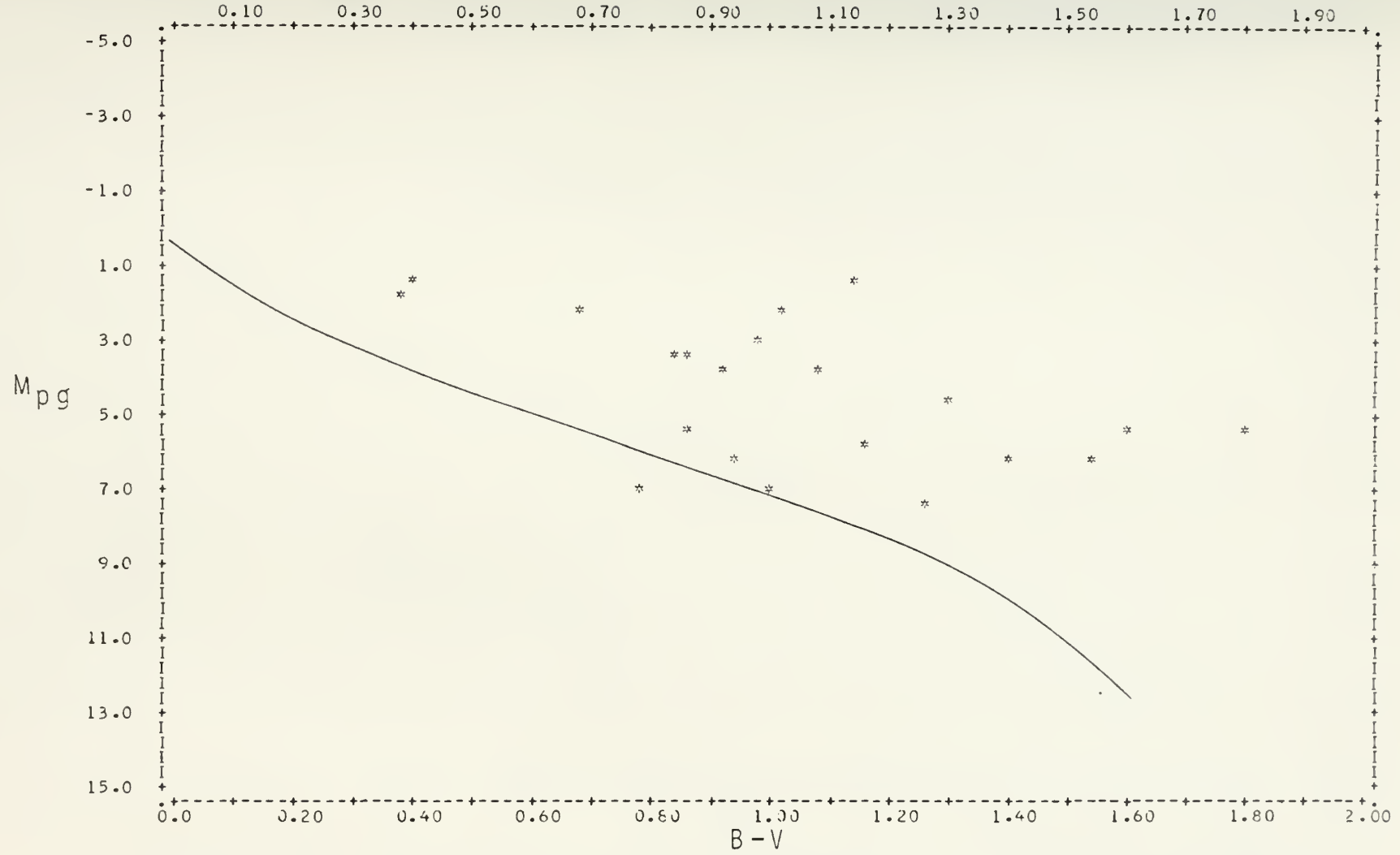

Figure 25- H-R diagram for the stars in the asterism Orion. Plotted values- 21.

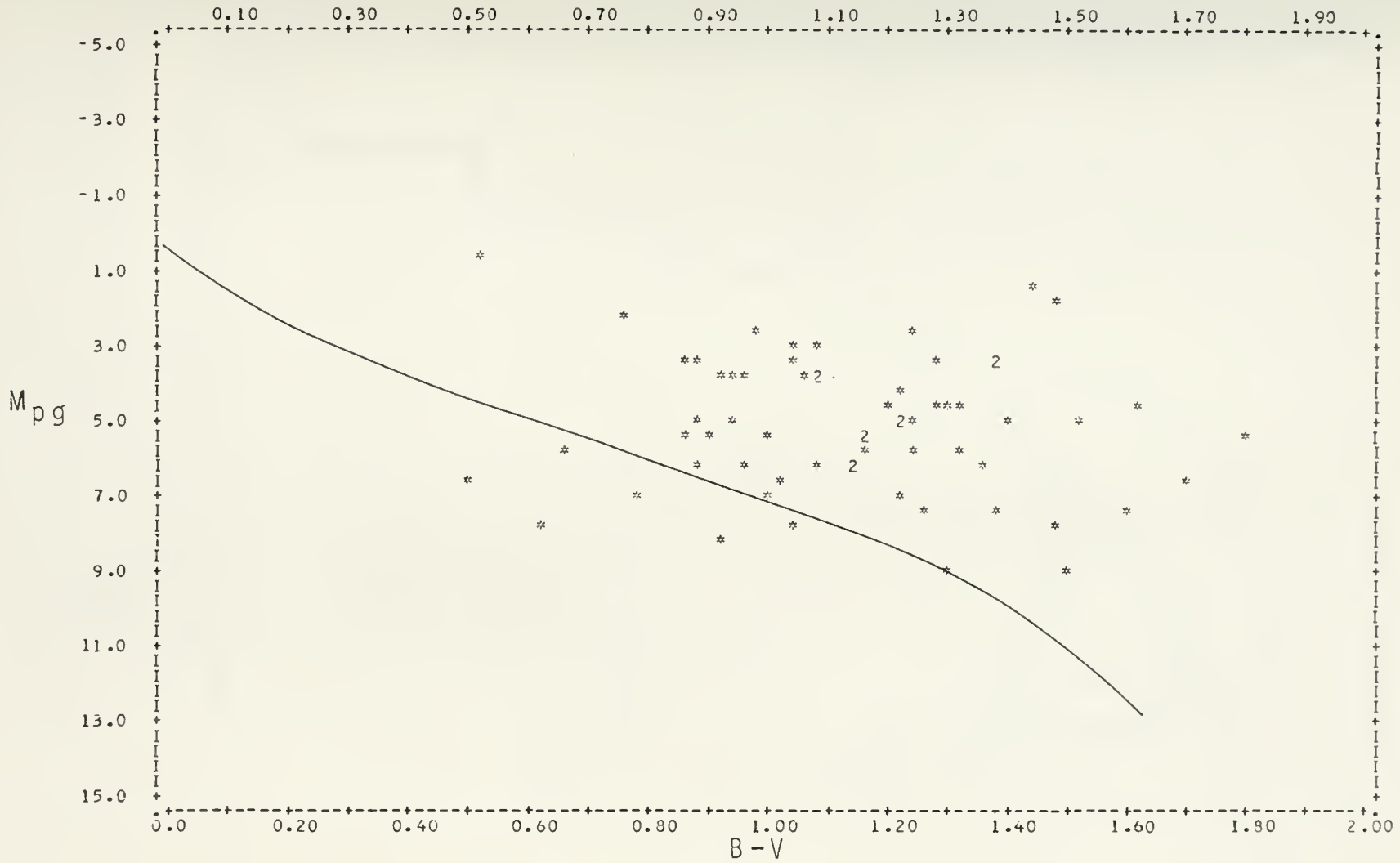

Figure 26- H-R diagram for all certain or possible T Tauri stars in the Catalog. Plotted values- 64.

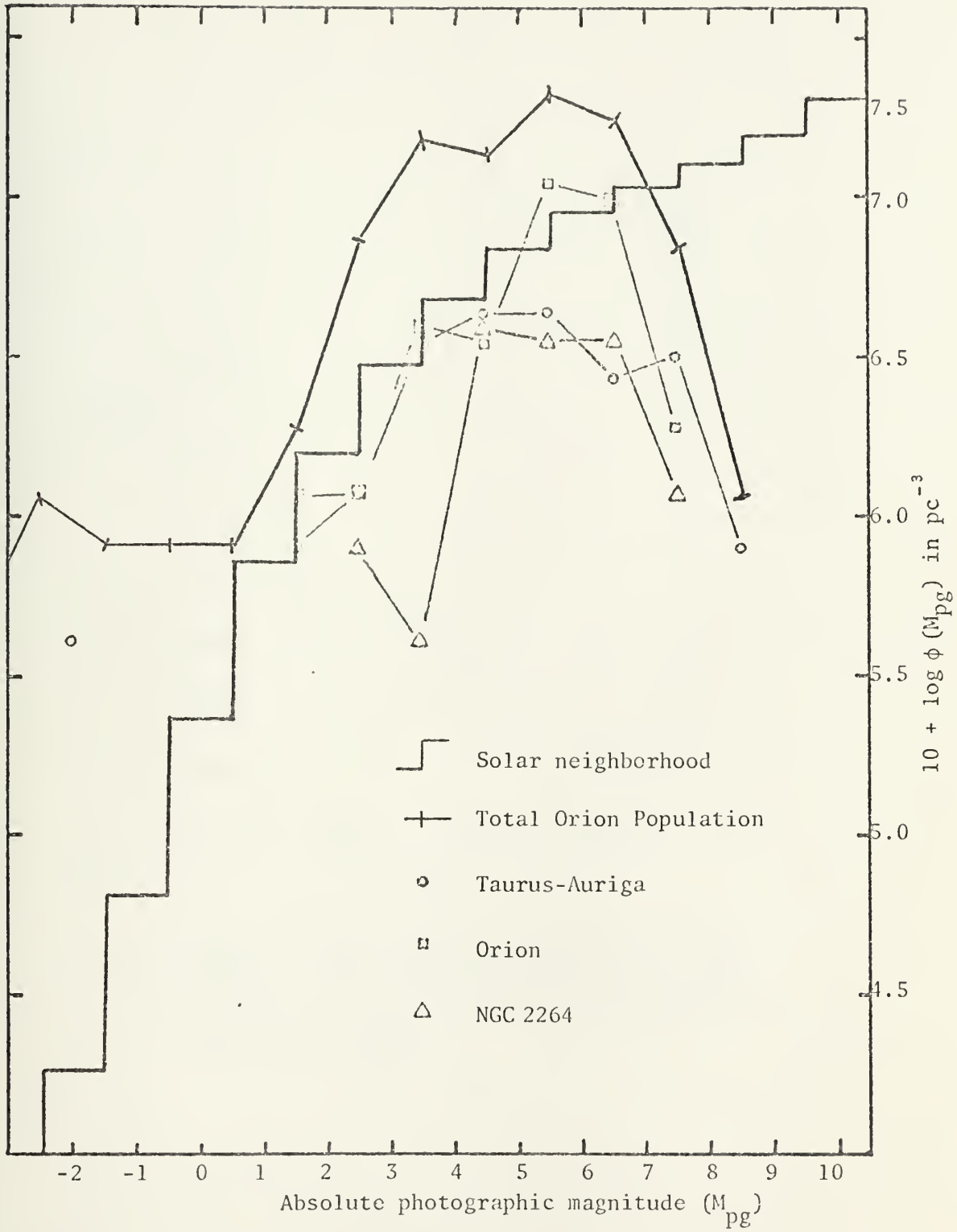

Figure 27. The Luminosity Functions, $\phi(M_{pg})$. The luminosity function for the solar neighborhood is adapted from Allen [1973]. The functions for the other four plots above have been normalized such that the number of stars in the total Orion Population is equal to the number found from integrating $\phi(M_{pg})$ in the solar neighborhood from $-2 \leq M_{pg} \leq 10$.

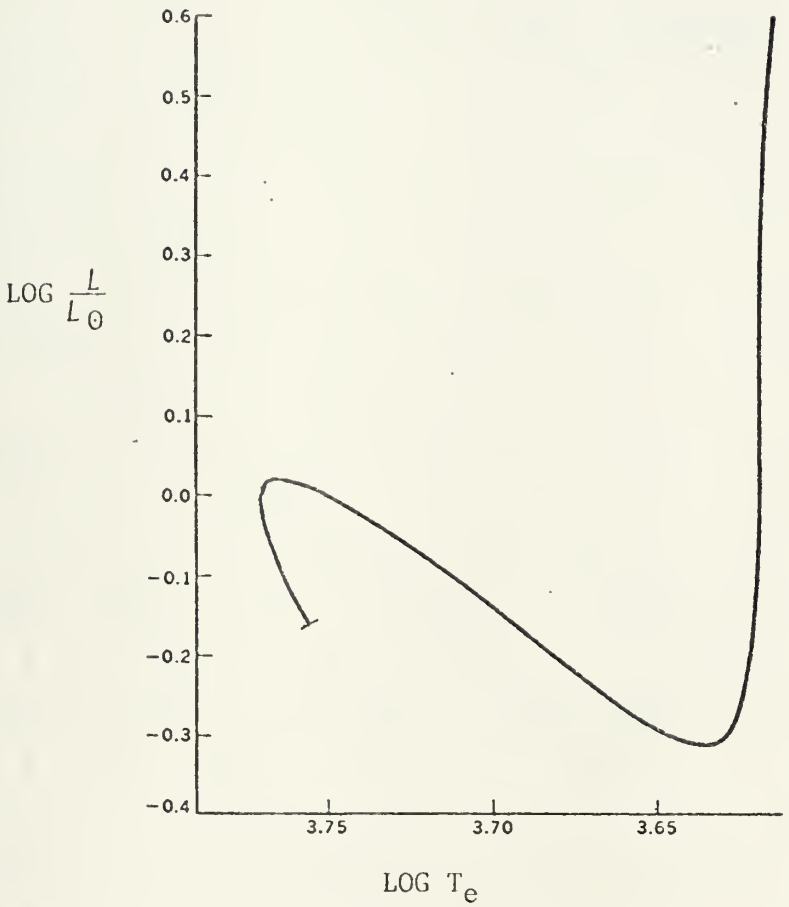

Figure 28. H-R diagram showing the Hayashi track for a one solar mass protostar. The bar at the tracks end marks the stars position on the main sequence. The figure is adapted from Clayton [1968].

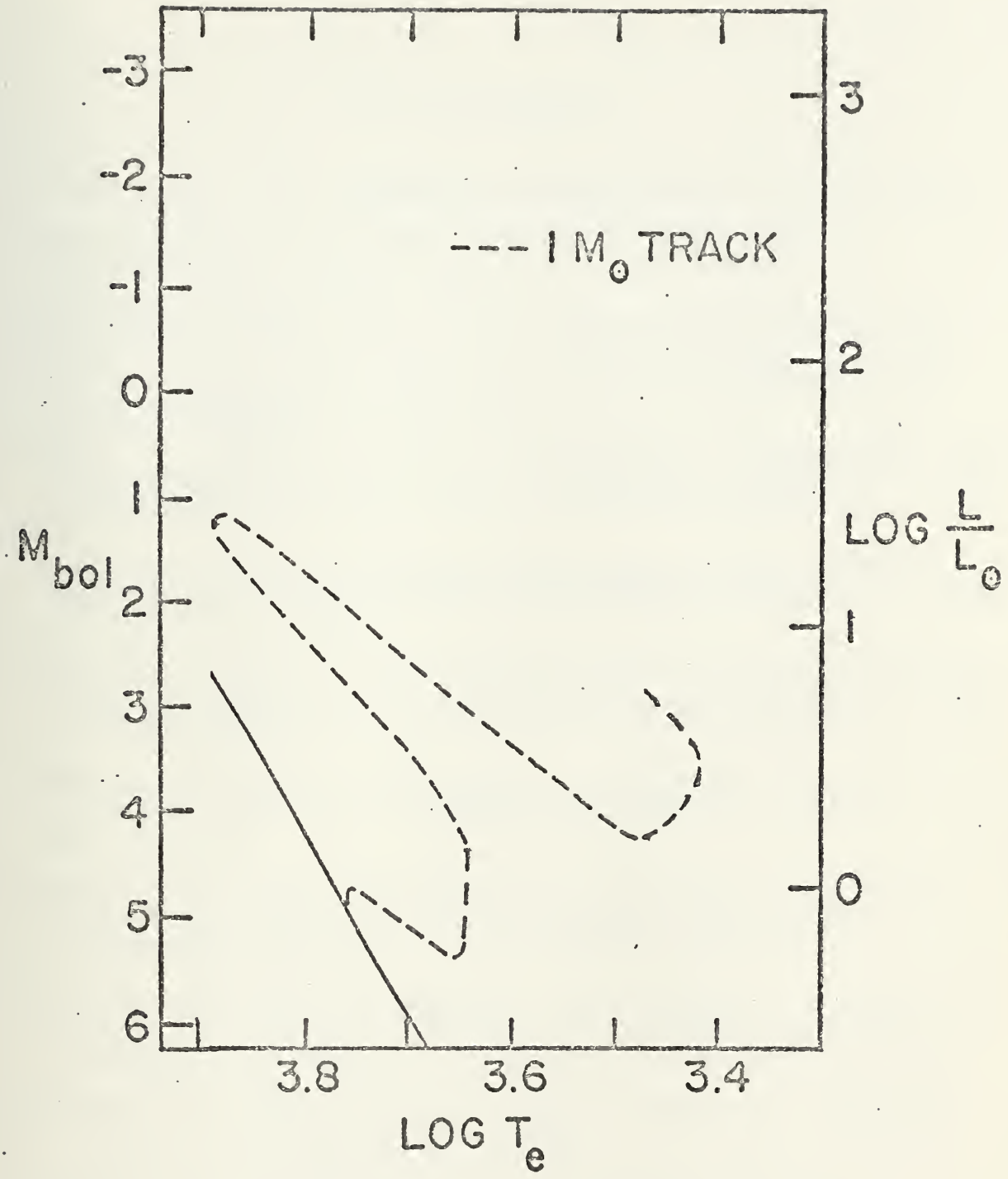

Figure 29. H-R diagram showing the Larson track for a one solar mass protostar. The solid line is the zero-age main sequence. The figure is adapted from Strom, Strom, and Grasdalen [1975].

LIST OF REFERENCES

Allen, C.W., 1973, Astrophysical Quantities, Athlone Press.

Ambartsumyan, V.A., 1958, Theoretical Astrophysics, pp. 479-480, Pergamon Press.

Buscombe, W, 1963, Mount Stromlo Observatory Mimeogram N6.

Clayton, D.D., 1968, Principles of Stellar Evolution and Nucleosynthesis, McGraw-Hill.

Cohen, M., 1973a, "Infrared Observations of Young Stars - II," Monthly Notices of the Royal Astronomical Society, V. 161, pp. 97-104.

Cohen, M., 1973b, "Infrared Observations of Young Stars - IV," Monthly Notices of the Royal Astronomical Society, V. 164, pp. 395-421, 1973b.

Cohen, M., 1974, "Infrared Observations of Young Stars - V," Monthly Notices of the Royal Astronomical Society, V. 169, pp. 257-272.

Herbig, G.H., 1957, "The Widths of Absorption Lines in T Tauri-like Stars," Astrophysical Journal, V. 125, pp. 612-613.

Herbig, G.H., 1960, "The Spectra of Be- and Ae-Type Stars Associated with Nebulosity," Astrophysical Journal Supplement Series, V. IV, No. 43, pp. 337

Herbig, G.H., 1962, "Properties and Problems of T Tauri Stars and Related Objects," Advances in Astronomy and Astrophysics, ed. Kopal, Z., V. 1, pp. 47-103, Academic Press.

Herbig, G.H., 1971, "The Spectrum of LkHα-101 in the Near-Infrared," Astrophysical Journal, V. 169, pp. 537-541.

Herbig, G.H. and Rao, N.K., 1972, "Second Catalog of Emission-Line Stars of the Orion Population," Astrophysical Journal, V. 174, pp. 401-423.

Imhoff, C.L. and Mendoza, E.E., 1974, "Computed Luminosities for T Tauri and Related Objects," Revista Mexicana de Astronomia y Astrofisica, V. 1, pp. 25-33.

Johnson, H.L. et al., 1961, Lowell Observatory Bulletin, V. 5, p. 133.

Johnson, H.L., 1968, "Interstellar Extinction," Nebulae and Interstellar Matter, V. VII, Stars and Stellar Systems, ed. Middlehurst, B.M. and Allen, L.H., pp. 167-220, University of Chicago Press.

Joy, A.H., 1945, "T Tauri Variable Stars," Astrophysical Journal, V. 102, pp. 168-195.

Kholopov, P.N., 1959, Astronomicheskii Zhurnal, V. 36, p. 294.

Kuhi, L.V., 1964, "Mass Loss from T Tauri Stars," Astrophysical Journal, V. 140, pp. 1409-1433.

Kuhi, L.V., 1966, "T Tauri Stars: A Short Review," Journal of the Royal Astronomical Society of Canada, V. 60, pp. 1-14.

Larson, R.B., 1969, "Numerical Calculations of the Dynamics of a Collapsing Proto-Star," Monthly Notices of the Royal Astronomical Society, V. 145, pp. 271-295.

Larson, R.B., 1972, "The Evolution of Spherical Protostars with Masses 0.25 $M_\odot$ to 10 $M_\odot$," Monthly Notices of the Royal Astronomical Society, V. 157, pp. 121-145.

Larson, R.B., 1973, "Processes in Collapsing Interstellar Clouds," Annual Reviews of Astronomy and Astrophysics, ed. Goldberg, L., V. 11, pp. 219-238, Annual Reviews Inc.

Mendoza, E.E., 1966, "Infrared Photometry of T Tauri Stars and Related Objects," Astrophysical Journal, V. 143, pp. 1010-1014.

Mendoza, E.E., 1968, "Infrared Excesses in T Tauri Stars and Related Objects," Astrophysical Journal, V. 151, pp. 977-989.

Nie, N., Bent, D.H., Hull, C.H., 1970, Statistical Package for the Social Sciences, McGraw-Hill Book Company.

Penston, M.V. and Hunter, J.K., 1975, "Further Observation of the Orion Cluster," Monthly Notices of the Royal Astronomical Society, V. 171, pp. 219-234.

Prentice, A.J.R., 1972, "Supersonic Convection and the Structure of T Tauri Stars," Proceedings of the Astronomical Society of Australia, V. 2, pp. 152-153.

Prentice, A.J.R., 1973, "On Turbulent Stress and the Structure of Young Convective Stars," Astronomy and Astrophysics, V. 27, pp. 237-248.

Rydgren, A.E., Strom, S.E., and Strom, K.M., 1975, "The Nature of the Objects of Joy: A study of the T Tauri Phenomenon," unpublished.

Strom, S.E. and Strom, K.M., 1973, "The Early Evolution of Stars - I," Sky and Telescope, V. 45, pp. 279-282.

Strom, S.E., Strom, K.M., and Grasdalen, G.L., 1975, "Young Stellar Objects and Dark Interstellar Clouds," Annual Reviews of Astronomy and Astrophysics, ed. Burbridge, G.R., V. 13, pp. 187-216, Annual Reviews Inc.

Walker, M.F., 1956, "Studies of Extremely Young Clusters. I.NGC 2264," Astrophysical Journal Supplement Series, V. II, No. 23, pp. 365-387.

Walker, M.F., 1972, "Studies of Extremely Young Clusters. VI," Astrophysical Journal, V. 175, pp. 89-116.

INITIAL DISTRIBUTION LIST

		No. Copies
1.	Defense Documentation Center Cameron Station Alexandria, Virginia 22314	2
2.	Library, Code 0212 Naval Postgraduate School Monterey, California 93940	2
3.	Department Chairman, Code 61 Department of Physics and Chemistry Naval Postgraduate School Monterey, California 93940	3
4.	Assoc. Professor W. B. Zeleny, Code 61 (Thesis Advisor) Department of Physics and Chemistry Naval Postgraduate School Monterey, California 93940	1
5.	Dr. William Bruce Weaver (Thesis Advisor) Monterey Institute for Research in Astronomy Bin 568 Carmel Valley, California 93924	1
6.	Lt. Joe Lee Frank III, USN USS Sacramento (AOE-1) FPO San Francisco California 96601	1